# Data assimilation and observation operators

ATARRI

Funded by the European Union

GA No 101160258

Emanuele Emili, Jeronimo Escribano

ERATOSTHENES CENTRE OF EXCELLENCE
BSC Barcelona Supercomputing Center Centro Nacional de Supercomputación
GRASP
ARMINES
MINES PARIS
PSL
Ciências ULisboa
FCiências.ID
pmod wrc

# Table of contents

- Basic concepts on Data Assimilation (DA)
- Variational and ensemble methods
- Mineral dust assimilation
  - The observation operator
  - Commonly assimilated observations
  - Example: the BSC DA implementation
  - Ongoing developments on dust and aerosols DA
- Final remarks

# What is data assimilation

- The process of objectively adapting the model state to observations in a statistically optimal way taking into account model and observation errors
- Concepts started to be developed in the 50s when first numerical weather predictions became possible
- More widespread adoption starting during the satellite era in the 70s
- Currently one of the major driver of weather forecasts improvements and applied to many other fields (ocean, land, atmospheric composition …)

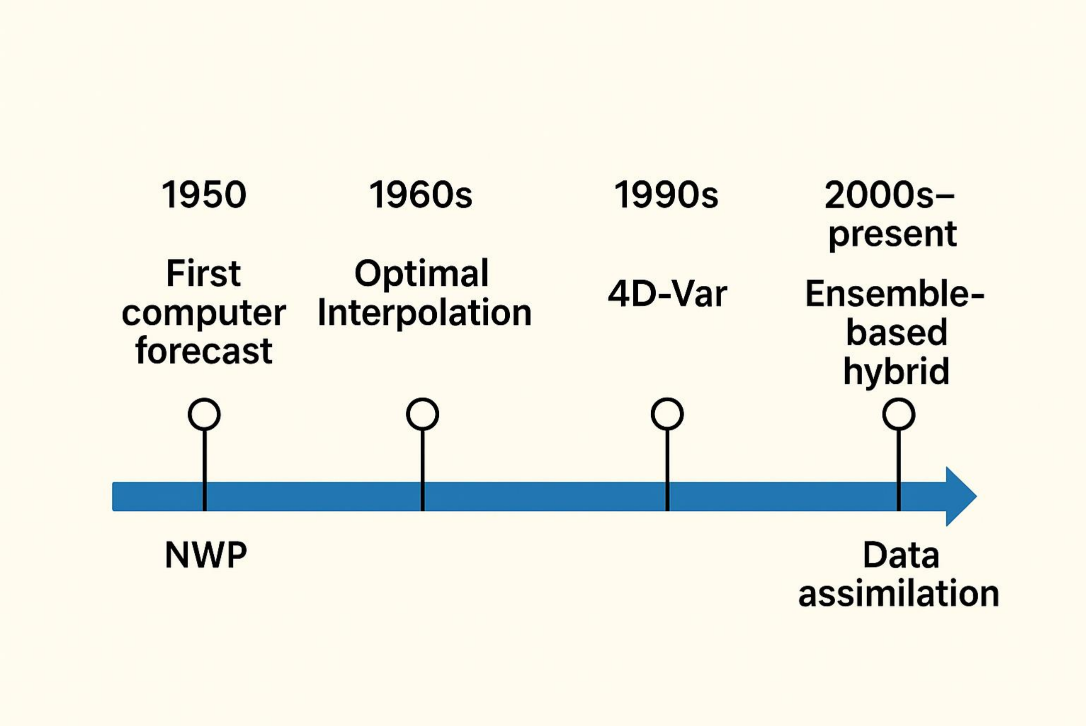

# Data assimilation in meteorology

https://www.ecmwf.int/sites/default/files/elibrary/81650-fifty-years-of-data-assimilation-at-ecmwf.pdf

Forecast skill changes of various models, including ECMWF's IFS, AIFS and ERA5. The figure shows the lead time at which the anomaly correlation of 500 hPa geopotential height over the northern hemisphere extratropics falls below 85%

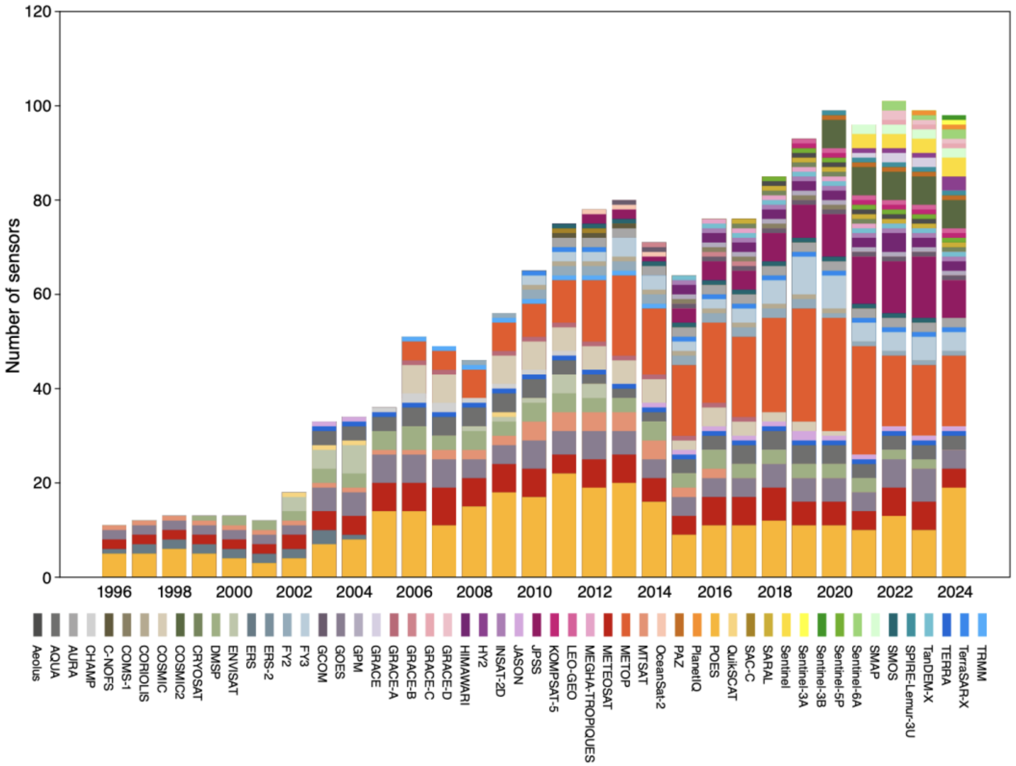


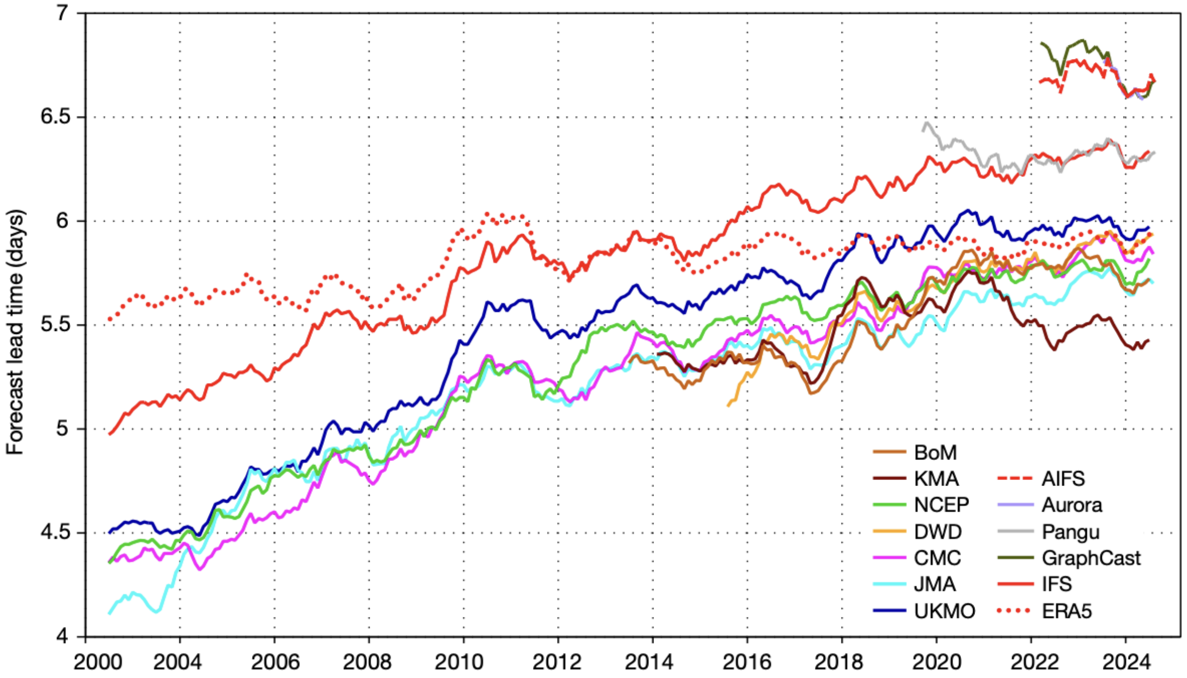

# What is data assimilation: demonstration

## Problem

Suppose you want to estimate the temperature of this room given:

a) A prior estimate: $T_b$ (e.g. based on your feeling)
b) A thermometer: $T_o$
c) The true (unknown) temperature $T_t$

but …

1. The prior estimate is affected by an error $\varepsilon_b = T_b - T_t$
2. The thermometer value is affected by an error $\varepsilon_o = T_o - T_t$
3. $\varepsilon_b$ and $\varepsilon_o$ are random variables

# What is data assimilation: demonstration

## Additional hypotheses

a) The statistical properties of the errors $\varepsilon_b$ and $\varepsilon_o$ are known

b) The errors are unbiased: $\overline{\varepsilon_b} = \overline{\varepsilon_o} = 0$

c) The errors are uncorrelated: $\overline{\varepsilon_b \varepsilon_o} = 0$

d) We look for a solution which is a linear combination of prior and measured temperature: $T_a = \alpha T_o + \beta T_b + \gamma$

# What is data assimilation: demonstration

## Let's do some algebra

- We were looking for a solution as $T_a = \alpha T_o + \beta T_b + \gamma$
- By substituting $T_a = \alpha(T_t + \varepsilon_o) + \beta(T_t + \varepsilon_b) + \gamma$
- The error of our estimate is: $\varepsilon_a = T_a - T_t = (\alpha + \beta - 1)T_t + \alpha\varepsilon_o + \beta\varepsilon_b + \gamma$
- We want it to be unbiased: $\overline{\varepsilon_a} = 0$
- which implies $(\alpha + \beta - 1)T_t + \gamma = 0$
- and hence $(\alpha + \beta - 1) = 0$ and $\gamma = 0$
- which gives the Linear Unbiased Estimate:

$$T_a = \alpha T_o + (1 - \alpha)T_b$$

# What is data assimilation: demonstration

Let’s do some algebra

- We are looking for a good value of $\alpha$ to compute $T_a = \alpha T_o + (1-\alpha)T_b$
- We can compute its error $\varepsilon_a = T_a - T_t = \alpha\varepsilon_o + (1-\alpha)\varepsilon_b$
- and its variance (remember $\overline{\varepsilon_b\varepsilon_o} = 0$):

$$\overline{\varepsilon_a^2} = \alpha^2\overline{\varepsilon_o^2} + (1-\alpha)^2\overline{\varepsilon_b^2}$$

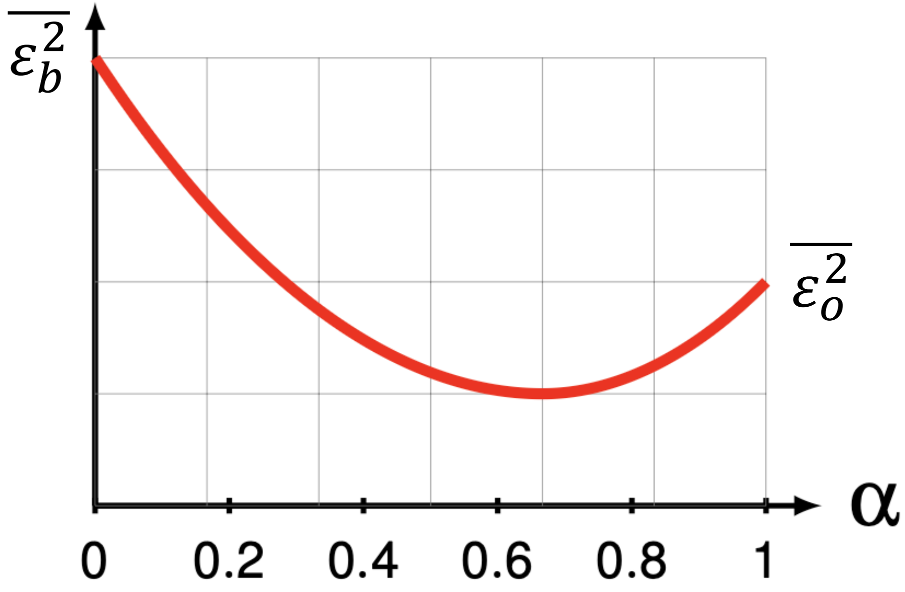


ERATOSTHENES CENTRE OF EXCELLENCE | BSC Barcelona Supercomputing Center Centro Nacional de Supercomputación | GRASP | ARMINES | MINES PARIS | PSL | Ciências ULisboa | FCiências.ID | pmod wrc

# What is data assimilation: demonstration

## Remarks

- For $0 \leq \alpha \leq 1, \overline{\varepsilon_a^2} \leq \max(\overline{\varepsilon_o^2}, \overline{\varepsilon_b^2})$
- The minimum is found for $\alpha = \frac{\overline{\varepsilon_b^2}}{\overline{\varepsilon_b^2}+\overline{\varepsilon_o^2}}$
- the analysis variance is $\overline{\varepsilon_a^2} = \frac{\overline{\varepsilon_b^2}^2}{\left(\overline{\varepsilon_b^2}+\overline{\varepsilon_o^2}\right)^2}\overline{\varepsilon_o^2} + \frac{\overline{\varepsilon_o^2}^2}{\left(\overline{\varepsilon_b^2}+\overline{\varepsilon_o^2}\right)^2}\overline{\varepsilon_b^2}$
- and the analysis is

$$T_a = \frac{\overline{\varepsilon_b^2}}{\overline{\varepsilon_b^2} + \overline{\varepsilon_o^2}} T_o + \frac{\overline{\varepsilon_o^2}}{\overline{\varepsilon_b^2} + \overline{\varepsilon_o^2}} T_b$$

$$\overline{\varepsilon_a^2} = \alpha^2\overline{\varepsilon_o^2} + (1-\alpha)^2\overline{\varepsilon_b^2}$$

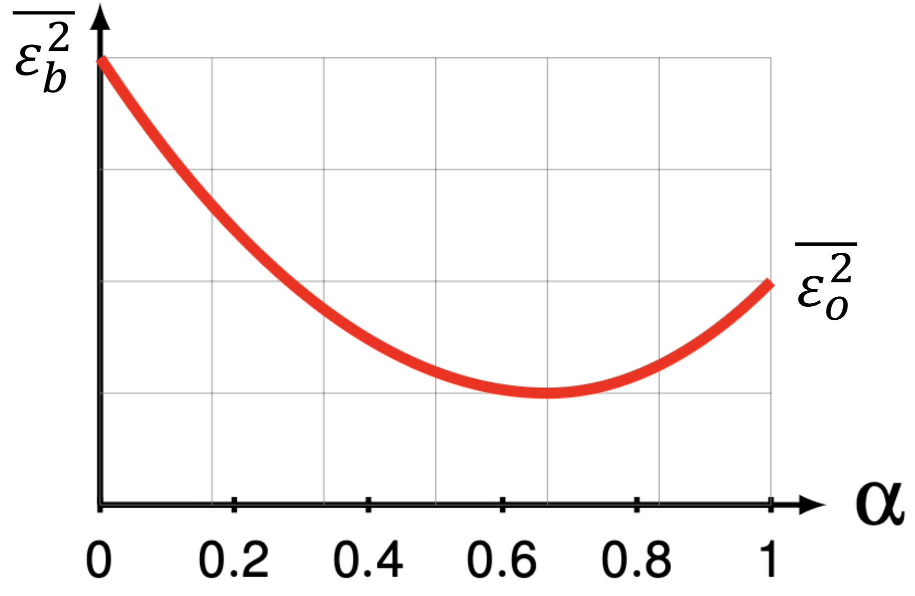

# What is data assimilation: definitions

Now let's extrapolate to multiple dimensions…

Suppose you want to estimate the state of a system identified by the vector $\boldsymbol{x}$:

a) With a prior estimate $\boldsymbol{x}_b$ (e.g. a model forecast) and corresponding errors $\boldsymbol{\varepsilon}_b$
b) A set of observations identified by the vector $\boldsymbol{y}_o$ and corresponding errors $\boldsymbol{\varepsilon}_o$
c) An observation operator $H(\boldsymbol{x})$ that maps the state of the model into the model equivalent of observations $\boldsymbol{y} = H(\boldsymbol{x})$

- Look again for a linear combination of the form $\boldsymbol{x}_a = \boldsymbol{x}_b + \mathbf{K}(\boldsymbol{y} - H(\boldsymbol{x}_b))$
- And ensure that $\boldsymbol{x}_a$ (the analysis) has the smallest possible variance $Trace\left(\overline{\boldsymbol{\varepsilon}_a \boldsymbol{\varepsilon}_a^T}\right)$

# What is data assimilation: general case

$$\boldsymbol{x}_a = \boldsymbol{x}_b + \mathbf{K}(\boldsymbol{y} - H(\boldsymbol{x}_b))$$

- Remember previously $T_a = \alpha T_o + (1-\alpha)T_b = T_b + \alpha(T_o - T_b)$
- $K$ is called *gain matrix* and $\boldsymbol{y} - H(\boldsymbol{x}_b)$ is called *innovation*
- ➢ Further assume errors small enough so that $H(\boldsymbol{x}_b) = H(\boldsymbol{x}_t) + \mathbf{H}\boldsymbol{\varepsilon}_b + O(\boldsymbol{\varepsilon}_b^2)$
- ➢ and repeating similar steps as in scalar example gives:

$$\mathbf{K} = \overline{\boldsymbol{\varepsilon}_b \boldsymbol{\varepsilon}_b^T}\mathbf{H}^T\left[\mathbf{H}\overline{\boldsymbol{\varepsilon}_b \boldsymbol{\varepsilon}_b^T}\mathbf{H}^T + \overline{\boldsymbol{\varepsilon}_o \boldsymbol{\varepsilon}_o^T}\right]^{-1}$$

or using more familiar notation for error covariances $\mathbf{P^b} = \overline{\boldsymbol{\varepsilon}_b \boldsymbol{\varepsilon}_b^T}$ $\mathbf{R} = \overline{\boldsymbol{\varepsilon}_o \boldsymbol{\varepsilon}_o^T}$

$$\mathbf{K} = \mathbf{P^b}\mathbf{H}^T\left[\mathbf{H}\mathbf{P^b}\mathbf{H}^T + \mathbf{R}\right]^{-1}$$

# Data assimilation: general case

$$\boldsymbol{x}_a = \boldsymbol{x}_b + \mathbf{P^b H}^T\left[\mathbf{H P^b H}^T + \mathbf{R}\right]^{-1}(\boldsymbol{y} - H(\boldsymbol{x}_b))$$

- This equation can be derived also from statistical considerations (Bayes theorem, under gaussian errors hypothesis)
- In real application scenarios the size of state and observation vectors is too large ($10^8$ or more) to inverse such matrices let so storing them in computer memory
- Error covariances must be assigned somehow
- When dealing with time evolving applications (e.g. atmospheric forecasts) prior errors should evolve as well with the state


Asch,Bocquet,Nodet 2016

# Temporal evolution

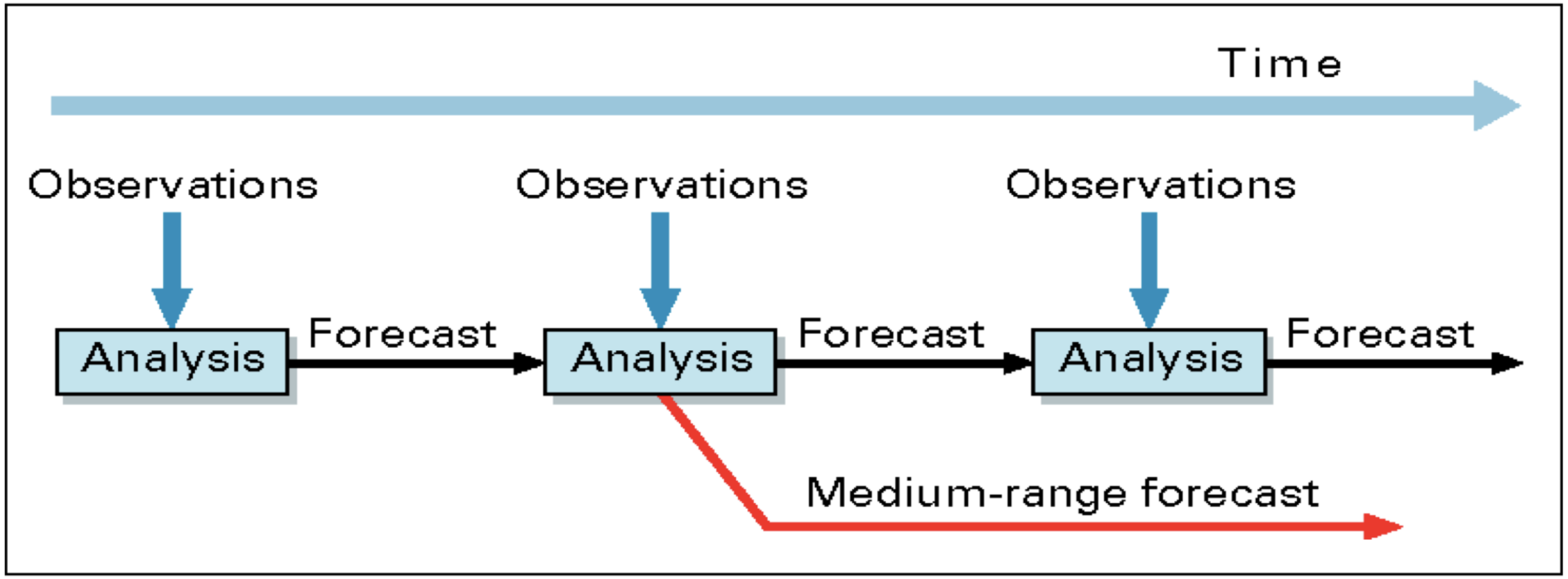

# Ensemble Kalman Filters

**Key ideas:**

- Approximate the prior error covariance with a sample of *M* Monte-Carlo model simulations (ensemble):

$$\mathbf{P}^{\mathbf{b}} \approx \frac{1}{M-1}\sum_m (\boldsymbol{x}_b^m - <\boldsymbol{x}_b^m>)(\boldsymbol{x}_b^m - <\boldsymbol{x}_b^m>)^T = \mathbf{X}_b\mathbf{X}_b^T$$

- Compute an ensemble of analysis states at each observation step
- Evolve the error covariances between observation steps

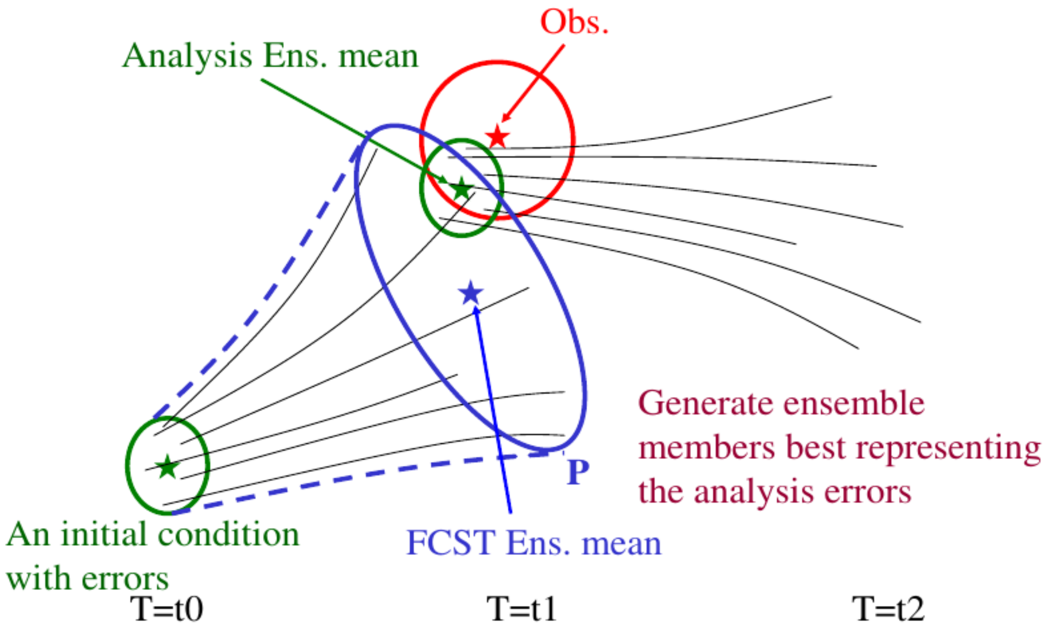


(fig. courtesy of Takemasa Miyoshi)

# Ensemble Kalman Filter

Key advantages:

- Is relatively simple to implement, only needed ingredients are the numerical forecast model and the observation operator
- The error covariances are in accordance with the state of the system
- Can be easily parallelized in the ensemble space (highly scalable)
- It produces uncertainty estimations as step of the algorithm
- Can account for uncertainties in model propagation

# Ensemble Kalman Filter

Key limitations:

- The limited size of the ensemble ($M << N$) introduces spurious correlations across grid points or model variables
  - This is handled by restricting the influence of distant observations (local analysis) or numerical tapering the raw ensemble covariance $\mathbf{P}_e^b$
  - But does not allow long range corrections
  - And it is not easy to *localize* indirect observations (e.g. satellite radiances)
- In some systems the ensemble spread tends to collapse over time due to the fit to observations (filter divergence)
  - This is addressed with inflating the spread of the ensemble or perturbing observations
- Costly
  - Current large models can afford generally less than 100 members
- Non linearities not well handled

# Ensemble Kalman Filters

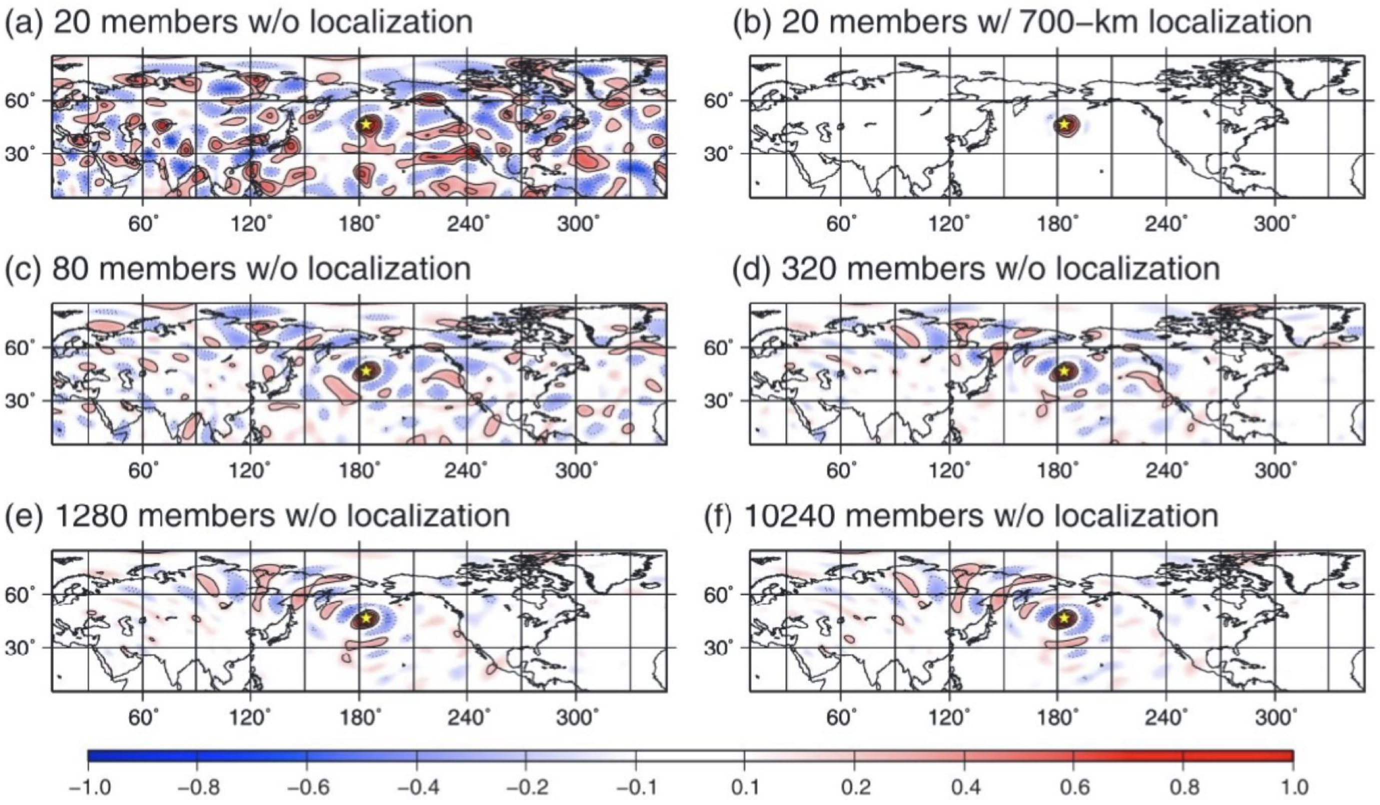


**Figure 4.** Similar to Figure 1 but at 00:00 UTC 18 January with the yellow star point at 46.389°N, 176.25°W and for different ensemble sizes ((a) 20, (c) 80, (d) 320, (e) 1280, and (f) 10,240 members) and (b) with localization for 20 members.

Miyoshi et al., 2014

# Local Ensemble Transform Kalman Filter

- Splits the model grid in subregions that can be processed in parallel
- Search for a solution using only local observations within a certain radius from each grid point (allows matrix inversions)
- Search for a solution in the space of the ensemble (generally smaller than the model state)

● Analysed grid point

◆ Local observations

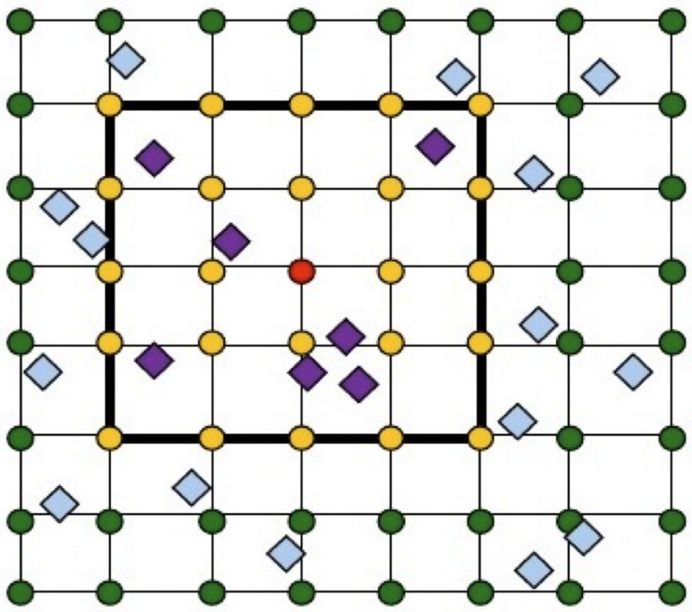

Hunt et al. 2007

# Variational methods: 3D-Var

- Rewrite the linear unbiased estimate as

$$\boldsymbol{x}_a = \boldsymbol{x}_b + \left[\mathbf{P^b}^{-1} + \mathbf{H}^T\mathbf{R}^{-1}\mathbf{H}\right]^{-1}\mathbf{H}^T\mathbf{R}^{-1}(\boldsymbol{y} - H(\boldsymbol{x}_b))$$

- And find $\delta\boldsymbol{x}_{\boldsymbol{a}} = \boldsymbol{x}_a - \boldsymbol{x}_b$ which solves the following linear system of the form $\mathbf{A}\boldsymbol{x} = \boldsymbol{b}$:

$$\left[\mathbf{P^b}^{-1} + \mathbf{H}^T\mathbf{R}^{-1}\mathbf{H}\right]\delta\boldsymbol{x} = \mathbf{H}^T\mathbf{R}^{-1}(\boldsymbol{y} - H(\boldsymbol{x}_b))$$

- Turns out that this is also the solution that minimize the linearized version of the following generic cost function:

$$J(\boldsymbol{x}) = \frac{1}{2}(\boldsymbol{x} - \boldsymbol{x}_b)^T\mathbf{P^b}^{-1}(\boldsymbol{x} - \boldsymbol{x}_b) + \frac{1}{2}[\boldsymbol{y} - H(\boldsymbol{x})]^T\mathbf{R}^{-1}[\boldsymbol{y} - H(\boldsymbol{x})]$$

- Very efficient numerical algorithms exist to minimize such high dimensional functions iteratively, without need to ever compute and store the involved large matrices
- This procedure provides a global solution $\delta\boldsymbol{x}_{\boldsymbol{a}}$ which fits all observations at once

# Variational methods: 4D-Var

- Consider a temporal window of K time steps with observations distributed across them
- We look for the initial state $\boldsymbol{x}_a$ that fits all the observations across the window by minimizing an extended cost function

$$J(\boldsymbol{x}) = \frac{1}{2}(\boldsymbol{x} - \boldsymbol{x}_b)^T \mathbf{P}^{\mathbf{b}^{-1}}(\boldsymbol{x} - \boldsymbol{x}_b) + \frac{1}{2}\sum_{k=0}^{K}[\boldsymbol{y}_k - G_k(\boldsymbol{x})]^T \mathbf{R}_k^{-1}[\boldsymbol{y}_k - G_k(\boldsymbol{x})]$$

- The dynamical model is used to compute observation equivalent at the proper time:

$$G_k = H_k \circ \mathcal{M}_{t_0 \to t_k}$$

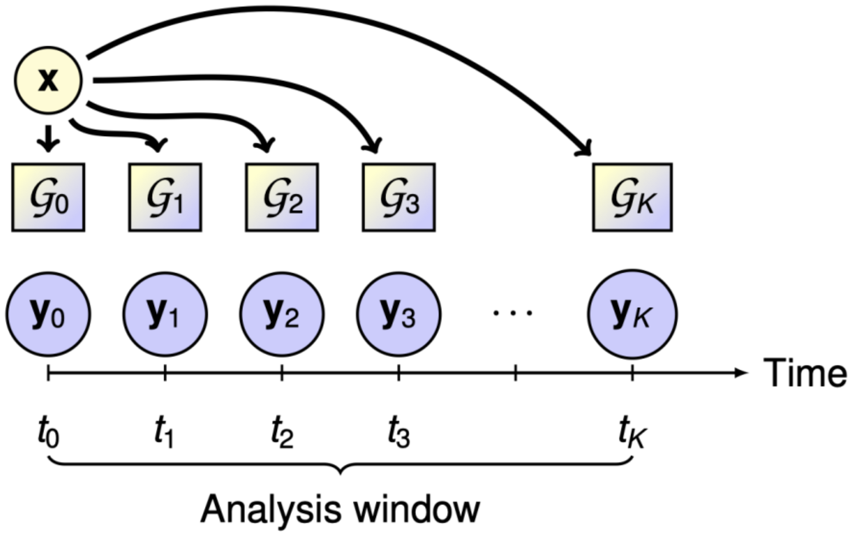


- Observations have an effect across the assimilation window
- The 4D-Var solution produces a smooth trajectory consistent with model physics

# Variational methods

Key advantages:

- Precise because based on explicit linearization of the observation operator (3D-Var) and of the model propagation (4D-Var)
- Produces a global analysis that accounts for all observations at once
- Can handle mild non-linearities in observation operators or models

Key limitations:

- Require linearized and adjoint models of the observation operator (3D-Var) and of the model (4D-Var)
- Require efficient numerical codes for covariance operators
- Do not provide flow-dependent prior errors estimation and do not return analysis covariances
- Accounting for potential errors in the model itself not straightforward

# Hybrid methods

- Hybrid methods are a family of assimilation algorithms that tries to address main issues of Ensemble and Variational methods alone.
- For example, Ensemble Data Assimilation (EDA) uses an ensemble of perturbed 4D-Var systems. This provides an estimate of uncertainty for the main unperturbed 4D-Var analysis.
- 4DEnVar replaces the model covariance matrix in the 4D-Var with an estimate done through an ensemble of model forecasts. This removes the need to maintain linearized and adjoint codes for the model, keeping the other perks of variational methods.

# Comparative table

| | Complexity / Maintenance effort | Numerical cost | Consistency of the analysis | Remarks |
|---|---|---|---|---|
| 3D-Var | Moderate | Low | Fair | • Temporal trajectories might not be physically consistent<br>• Formally very similar to atmospheric inversions (1D-Var) |
| 4D-Var | High | High | Good | • Better temporal consistence, more effective use of observations<br>• Needs linearized and adjoint codes of the model |
| EnKF | Low | High | Fair | • Only uses forward model and forward observation operator<br>• Comes with uncertainty estimation<br>• Affected by sampling noise |

# Examples: stratospheric $O_3$ assimilation

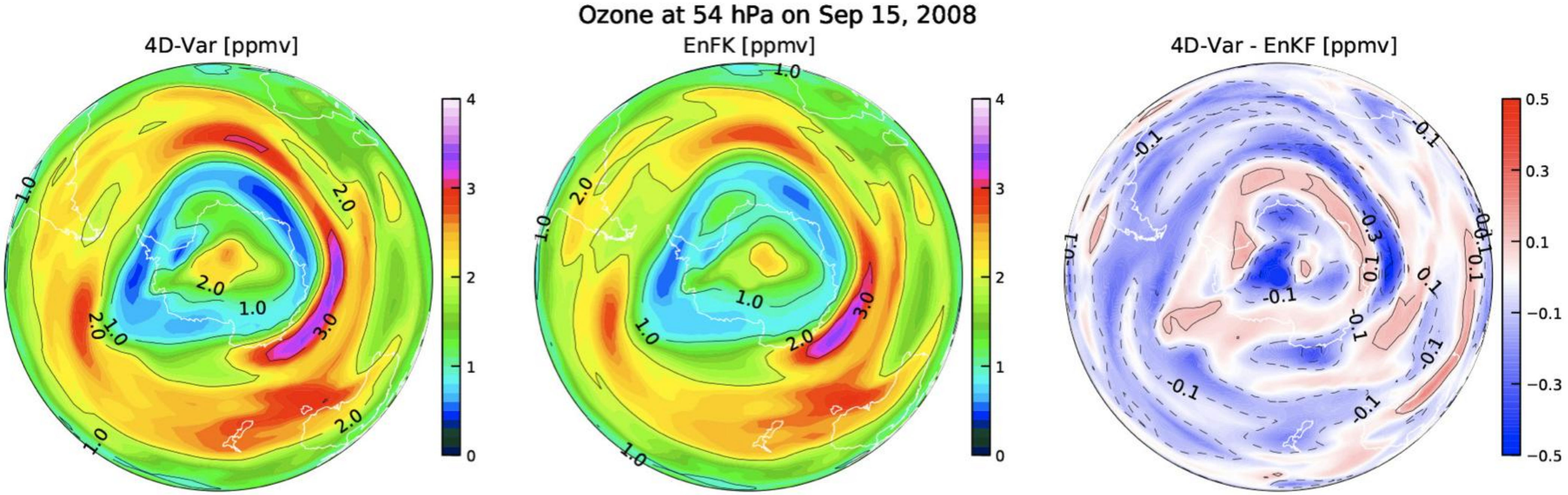


Skachko et al. (2014)

# Examples: $CO_2$ flux inversions

Liu et al. (2016)

- Data assimilation used to estimate $CO_2$ fluxes
- The impact of distant observations and error covariances is larger
- 4D-Var is found to produce more coherent fluxes over data sparse regions

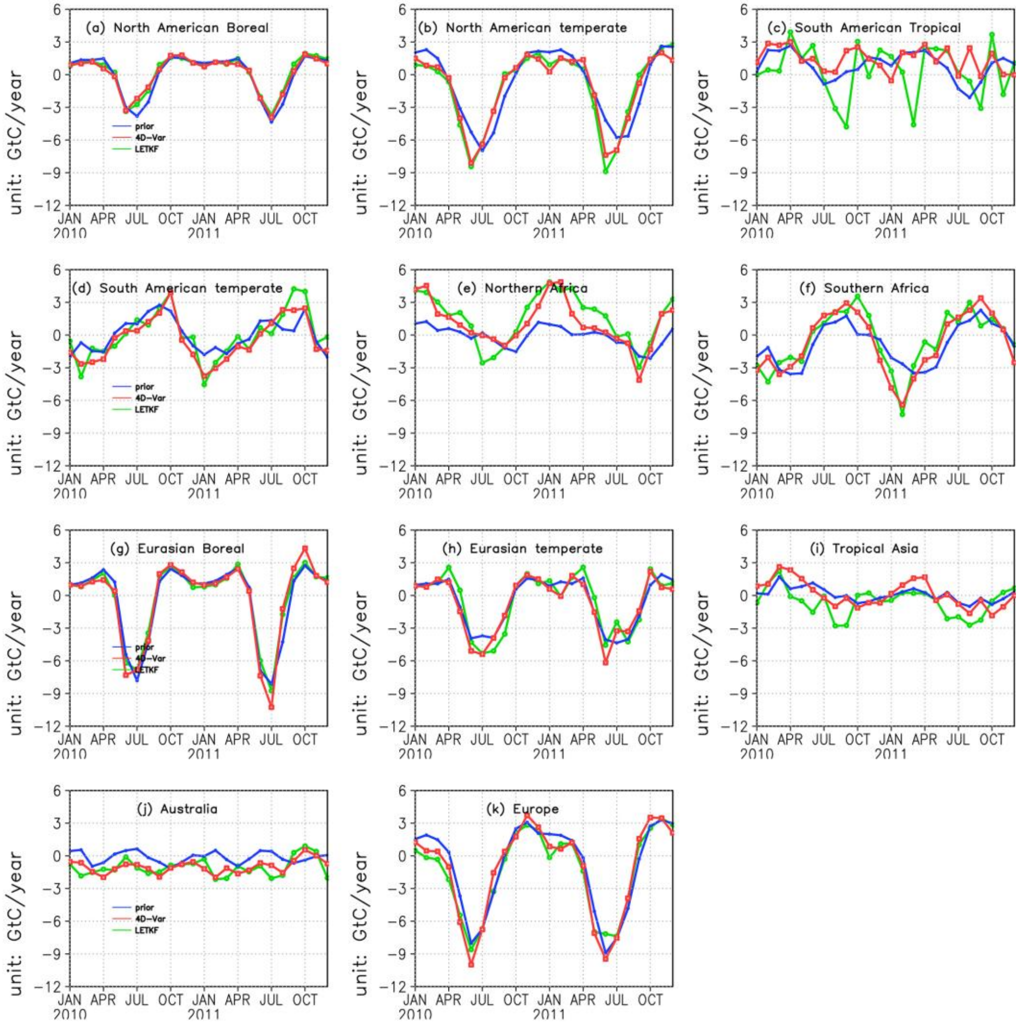

# Mineral dust assimilation: from observations to operations

# Mineral dust assimilation: key aspects

- A complex mixture of initial conditions and model errors

Initial conditions / transport / wet deposition errors dominate

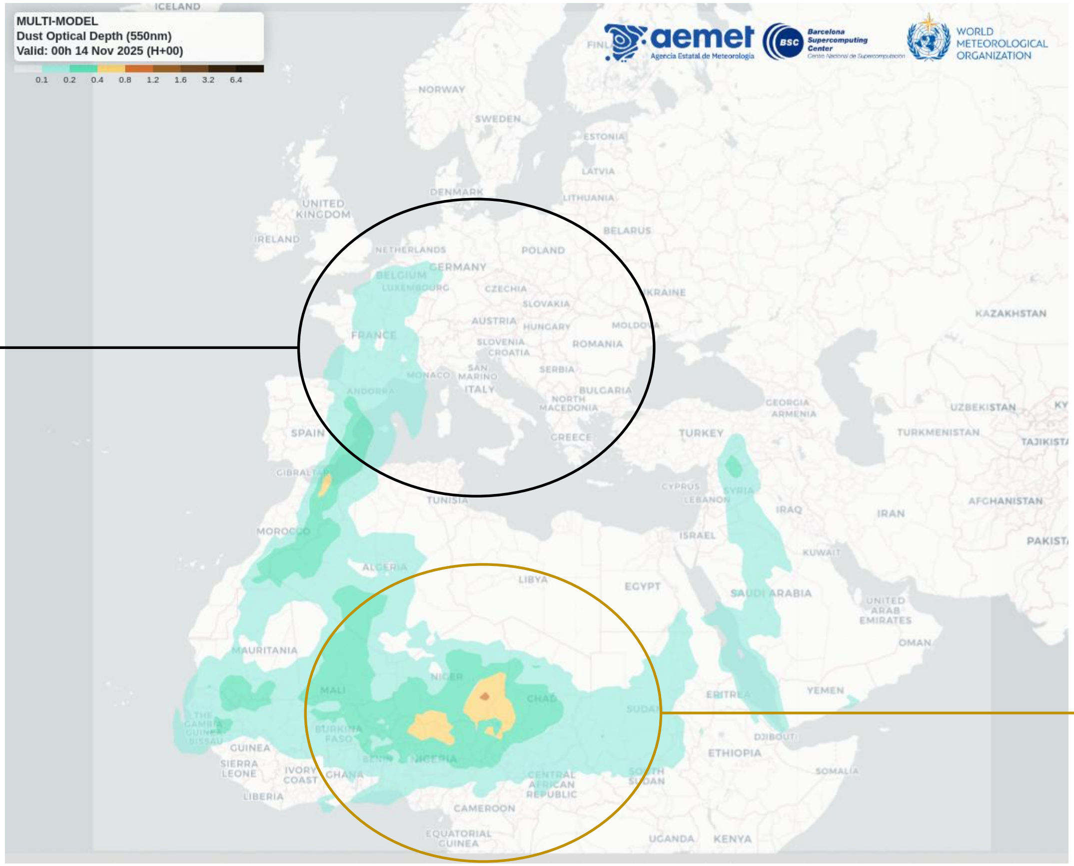


Emissions / dry deposition errors dominate

# Mineral dust assimilation: key aspects

- A complex mixture of initial conditions and model errors
- In most forecasting systems the total aerosols 3D mass concentrations is the DA state vector
- Typical assimilation windows range from 1 hour (3D-Var) to 24 hours (4D-Var, LETKF) with the final step used to reinitialize the follow-up forecast (up to 5 days range)

➢ Impact of assimilation decreases with forecast range

# Observations

| Sensor | Dust-related variables | Covered period | Resolution | Wavelength ($\mu$m) | Product type (O, R) | Open access (Y/N) | Main dust retrieval publications |
|---|---|---|---|---|---|---|---|
| AIRS | DOD | 2003–11 | Monthly | 0.55; 10 | O | Y | Peyridieu et al. (2010) |
| | Dust altitude | | | | O | | |
| | Effective radius | | 1° × 1° | | R | | |
| ATSR-2/AATSR | AOD | 1995–2012 | Daily | 0.55 | O | Y | Bevan et al. (2012), Poulsen et al. (2012), North (2002), Veefkind et al. (1998) |
| | Fine mode aerosol optical depth (FMAOD) | | 1° × 1° and 10 km × 10 km | | O | | |
| | DOD | | | | R | | |
| GOME-2 | AAI | 2007–present | Daily, monthly | 0.34–0.38 | O | Y | Tilstra et al. (2013) |
| | | | 1° × 1° | | | | |
| IASI | DOD | 2007–present | Twice a day, monthly | 0.55; 10; 11 | O | Y | Clarisse et al. (2019), Callewaert et al. (2019), Capelle et al. (2018), Klüser et al. (2015) |
| | Dust altitude/profile | | 12 km × 12 km | | O | | |
| | Dust parameters (size, mineralogy) | | | | R | | |
| MISR | AOD | 2002–present | Subdaily, daily, monthly, etc. | 0.55 | O | Y | Kahn et al. (2010), Martonchik et al. (2009) |
| | Aerosol typing | | 4.4 km × 4.4 km | | O | | |
| | DOD (nonspherical fraction) | | 0.5° × 0.5° | | O | | |
| MODIS dark target | AOD | 2000–present | 5 min, daily | 0.55 | O | Y | Levy et al. (2013) |
| | | | 3 km × 3 km | | O | | |
| | AE | | 10 km × 10 km | | R | | |
| | | | 1° × 1° | | | | |
| MODIS deep blue | AOD | 2000–present | 5 min, daily | 0.55 | O | Y | Hsu et al. (2004), Hsu et al. (2013), Gkikas et al. (2021) |
| | AE | | 3 km × 3 km | | O | | |
| | SSA | | 10 km × 10 km | | O | | |
| | DOD (obtained by synergy with external datasets) | | 1° × 1° | | R | | |
| OMI | AOD | 2004–present | Subdaily, daily, 32 days | 0.35–0.50 | O | Y | Torres et al. (2013) |
| | AAI | | 13 km × 12 km (24 km) | | O | | |
| | SSA | | 0.25° × 0.25° | | O | | |
| | | | 1° × 1° | | | | |
| POLDER | AOD | 2005–13 | Daily, monthly, seasonally, yearly | 0.44–1.02 | O | Y | Dubovik et al. (2014) |
| | AE | | 6 km × 6 km | | O | | |
| | DOD (coarse) | | | | O | | |
| | SSA | | 0.1° × 0.1° | | O | | |
| | Aerosol mean layer altitude | | | | O | | |

| Sensor | Dust-related variables | Covered period | Resolution | Wavelength ($\mu$m) | Product type (O, R) | Open access (Y/N) | Main dust retrieval publications |
|---|---|---|---|---|---|---|---|
| SeaWIFs deep blue | AOD | 1997–2010 | Subdaily, daily, monthly | 0.55 | O | Y | Hsu et al. (2012), Sayer et al. (2012) |
| | AE | | 13.5 km × 13.5 km | | O | | |
| | SSA | | 0.5° × 0.5° | | O | | |
| | | | 1° × 1° | | | | |
| SEVIRI | AOD | 2004–present | Hourly, daily, monthly | 0.55 | O | Y | Luffarelli and Govaerts (2019), Clerbaux et al. (2017), Schepanski et al. (2007) |
| | FMAOD | | 4 km × 5 km | | R | | |
| | Dust index | | 0.1° × 0.1° | | R | | |
| | Dust RGB maps | | 1° × 1° | | O | | |
| SLSTR | AOD | 1995–2012 | Daily | 0.55 | O | Y | Bevan et al. (2012), Poulsen et al. (2012), North (2002), Veefkind et al. (1998) |
| | FMAOD | | 10 km × 10 km | | O | | |
| | | | 1° × 1° | | | | |
| TOMS | AOD | 1979–2004 | Subdaily, daily, monthly | 0.34–0.38 | O | Y | Torres et al. (1998), Torres et al. (2002) |
| | | | 50 km × 50 km | | | | |
| | AAI | | 1° × 1.5° | | | | |
| | | | 7 km × 3.5 km | | | | |
| TROPOMI | AAI | 2017–present | Subdaily | 0.34–0.38 | O | Y | Veefkind et al. (2012) |
| | | | 7 km × 3.5 km | | | | |
| ALADIN | Backscatter profiles | 2018–present | Daily | 0.355 | O | N | Flamant et al. (2007) |
| | Extinction profile | | | | O | | |
| CALIOP | Backscatter profiles | 2006–present | Daily, monthly | 0.532–1.064 | O | Y | Amiridis et al. (2013, 2015), Winker et al. (2009), Omar et al. (2009), Zheng et al. (2022) |
| | Depolarization profiles | | | | O | | |
| | Aerosol typing profiles | | | | O | | |
| | Dust/mixed dust layers | | | | O | | |
| | Pure dust extinction profiles | | | | R (post-processed) | | |
| | Pure DOD | | | | R (post-processed) | | |
| CATS | Backscatter profiles | 2015–17 | Daily | 1.064 | O | Y | McGill et al. (2015), Proestakis et al. (2019), Yorks et al. (2016) |
| | Depolarization profiles | | | | O | | |
| | Aerosol typing profiles | | | | O | | |

Mona, L., and Coauthors, 2023: Observing Mineral Dust in Northern Africa, the Middle East, and Europe: Current Capabilities and Challenges ahead for the Development of Dust Services. Bull. Amer. Meteor. Soc., 104, E2223–E2264, [https://doi.org/10.1175/BAMS-D-23-0005.1](https://doi.org/10.1175/BAMS-D-23-0005.1)

# Observation operator

Retrieved quantities

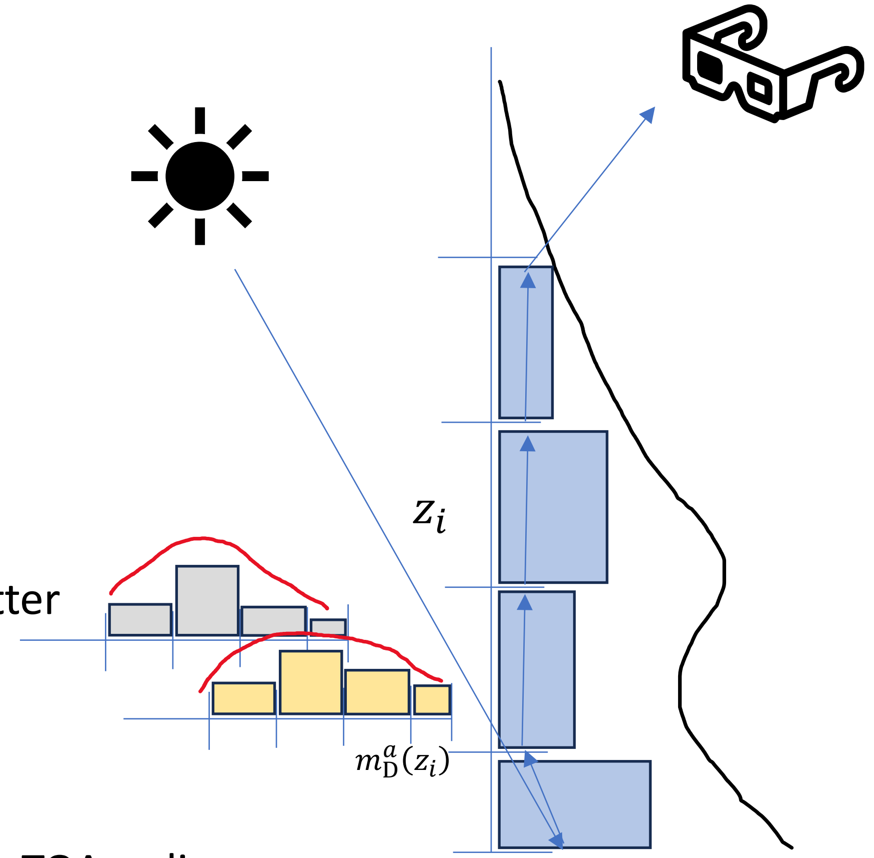


$$H(\boldsymbol{x}) = \sum_i \sum_a \sum_{\mathrm{D}} \underbrace{m_{\mathrm{D}}^{a}(z_i)\, C_{ext}^{a,\mathrm{D}}}_{\alpha(z_i)}(\lambda)$$

Optical depth

$$H(\boldsymbol{x}) = \sum_a \sum_{\mathrm{D}} \underbrace{m_{\mathrm{D}}^{a}(z_i)\, C_{back}^{a,\mathrm{D}}}_{\beta(z_i)}(\lambda)$$

Backscatter profile

$$H(\boldsymbol{x}) = K\beta(z)e^{-2\int_0^z \alpha(z)dz}$$

Attenuated backscatter

$$H(\boldsymbol{x}) = RTM(aero, gases, surf, sun\ and\ sat\ view\ angles)$$

TOA radiances

Raw Measurement

# Observation operator: assumptions and limits

- The observation operator should use same underlying assumptions on particle size, shape and optical properties as the forecast model
- Same dust concentrations can provide different optical depths
- And modeled PSD and optics are not necessarily the same used to retrieve dust properties from space or from ground instruments!

➢ Improving the fit with observations through DA does not ensure better dust concentrations

Particle size distribution

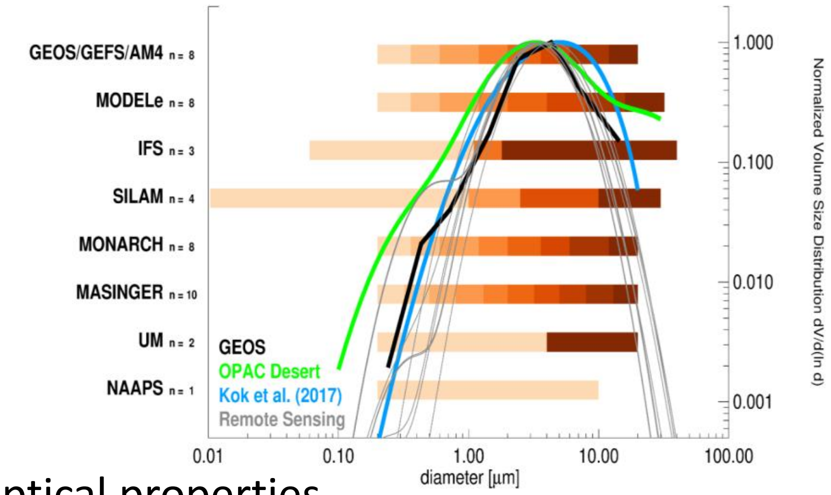


Dust optical properties

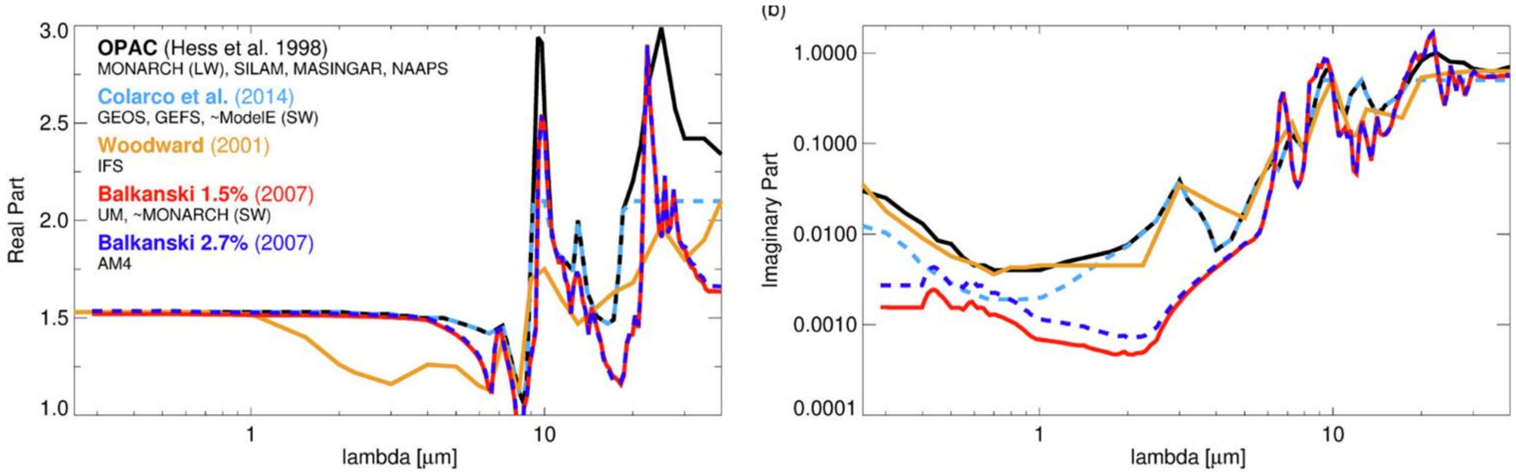


*Castellanos, P., et al. (2024). Mineral dust optical properties for remote sensing and global modeling: A review. In Remote Sensing of Environment (Vol. 303). Elsevier Inc. https://doi.org/10.1016/j.rse.2023.113982*

# Observations: polar orbiting

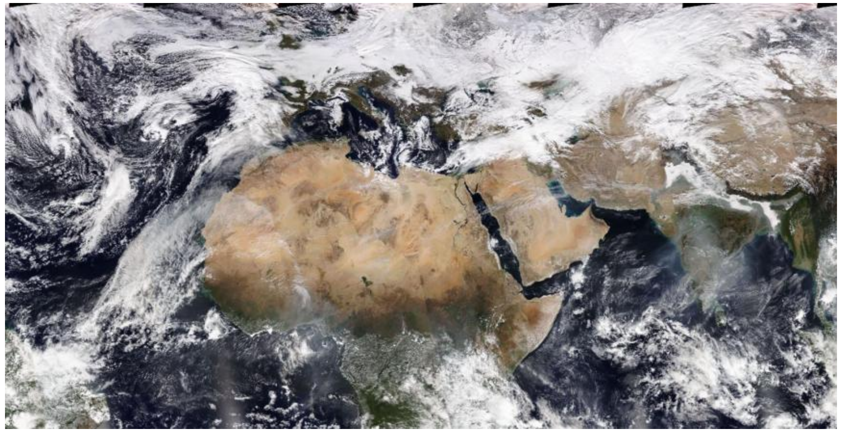

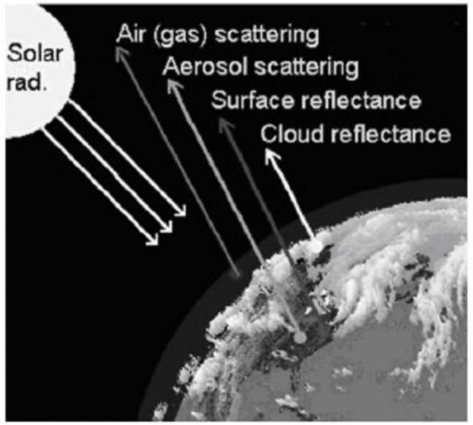


HSU ET AL.: ENHANCED DEEP BLUE AEROSOL RETRIEVAL

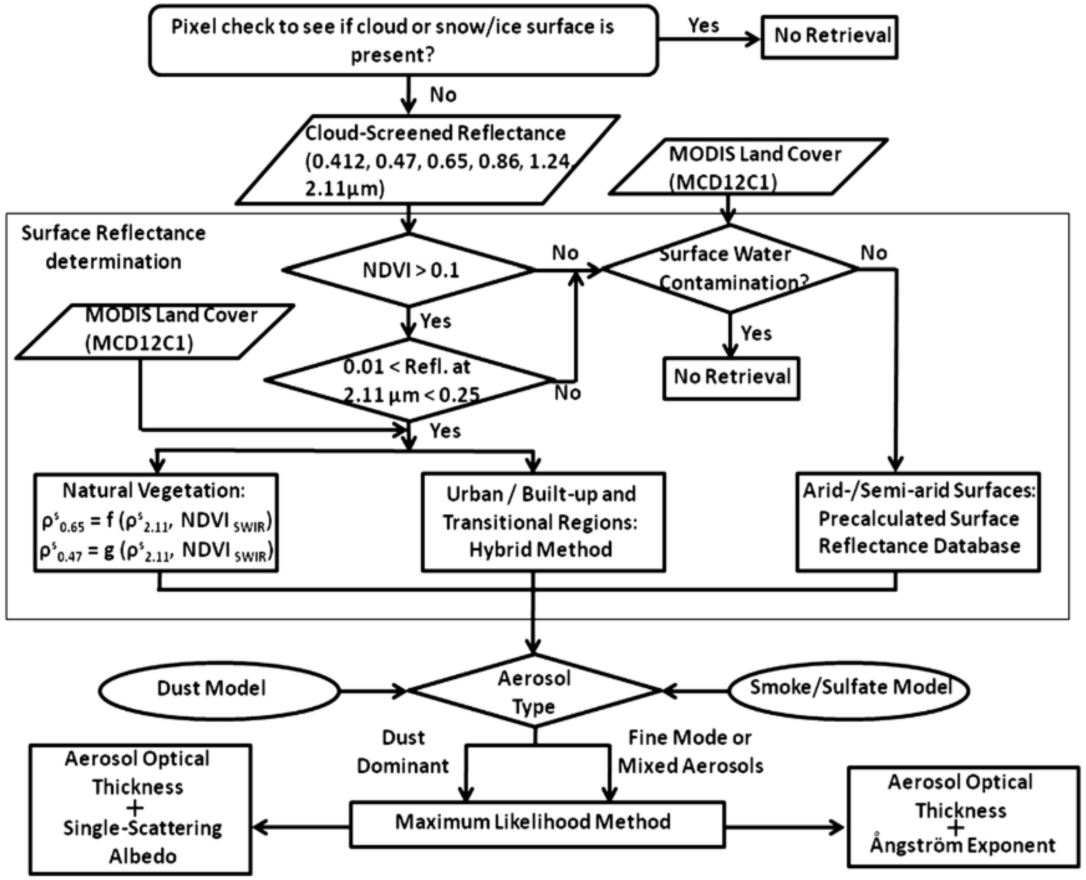


**Figure 1.** Flowchart of the enhanced MODIS Deep Blue algorithm.

# Observations: polar orbiting

- The Deep Blue algorithm dust flag allows for screening of dust contaminated pixels
  - ➢ Provides a simple approach to limit undesired contamination of other aerosols when only dust is the control variable
  - ○ But strongly reduces the number of assimilated observations
- Other approaches exist to derive Dust Optical Depth, based on retrieved Angstrom exponent and Single Scattering Albedo (Ginoux, 2012)

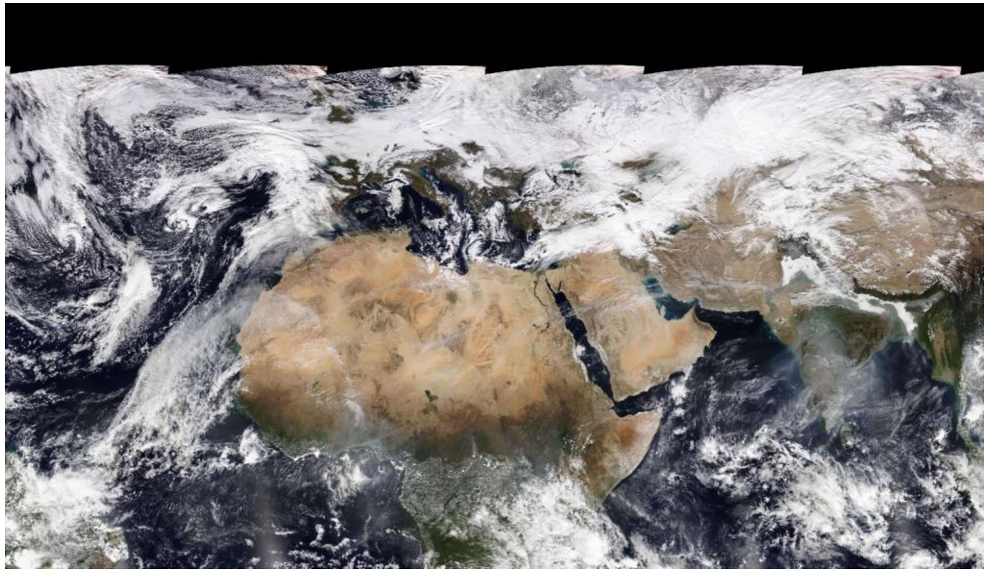

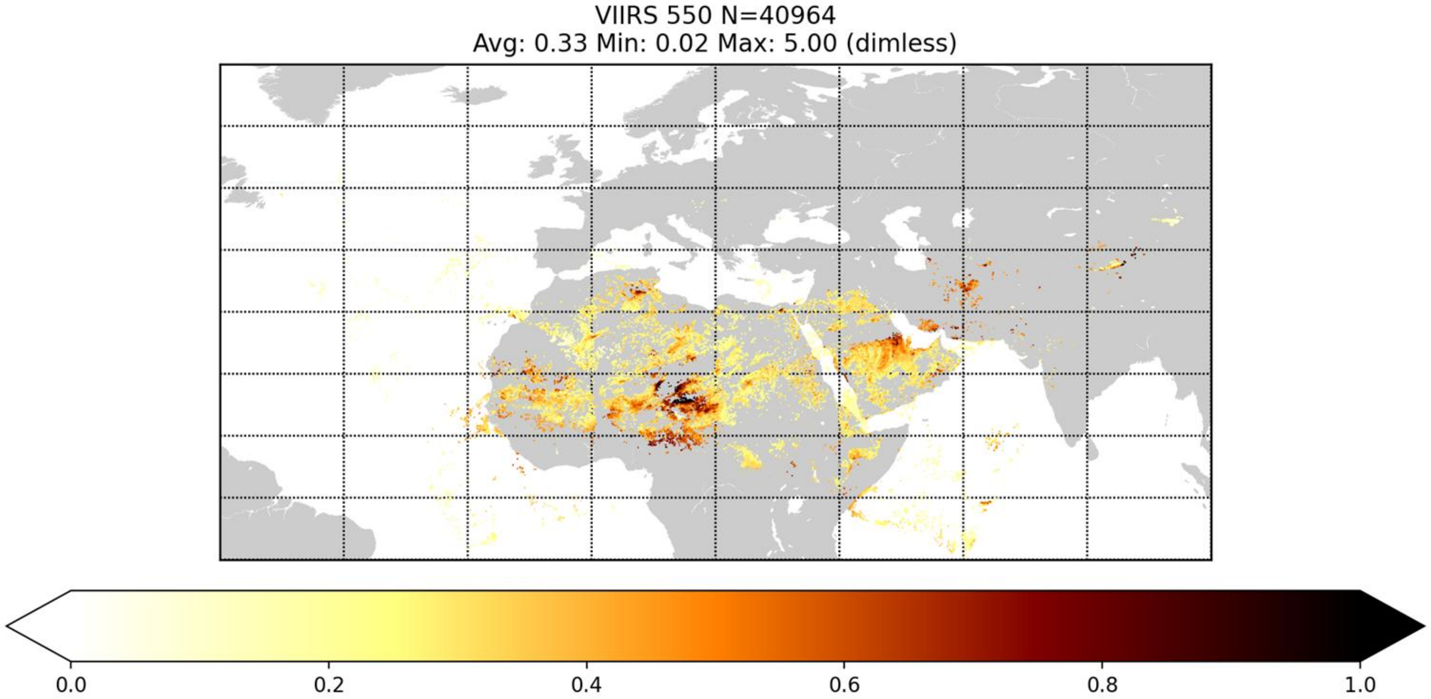

# Observations: GEO-ring

Ceamanos et al (2021)

Meteorological geostationary platforms provide very frequent observations (15 min), but less spectral channels and at lower spatial resolution:

- Only total optical depth retrieval generally accessible
- The high frequency is needed to disentangle surface and aerosols signal, output AOD is daily
- Less accurate retrievals than with polar orbiting sensors (also due to less favorable observing angles)

Sentinel-4 will improve spectral and spatial resolution, but main dust sources will not be covered

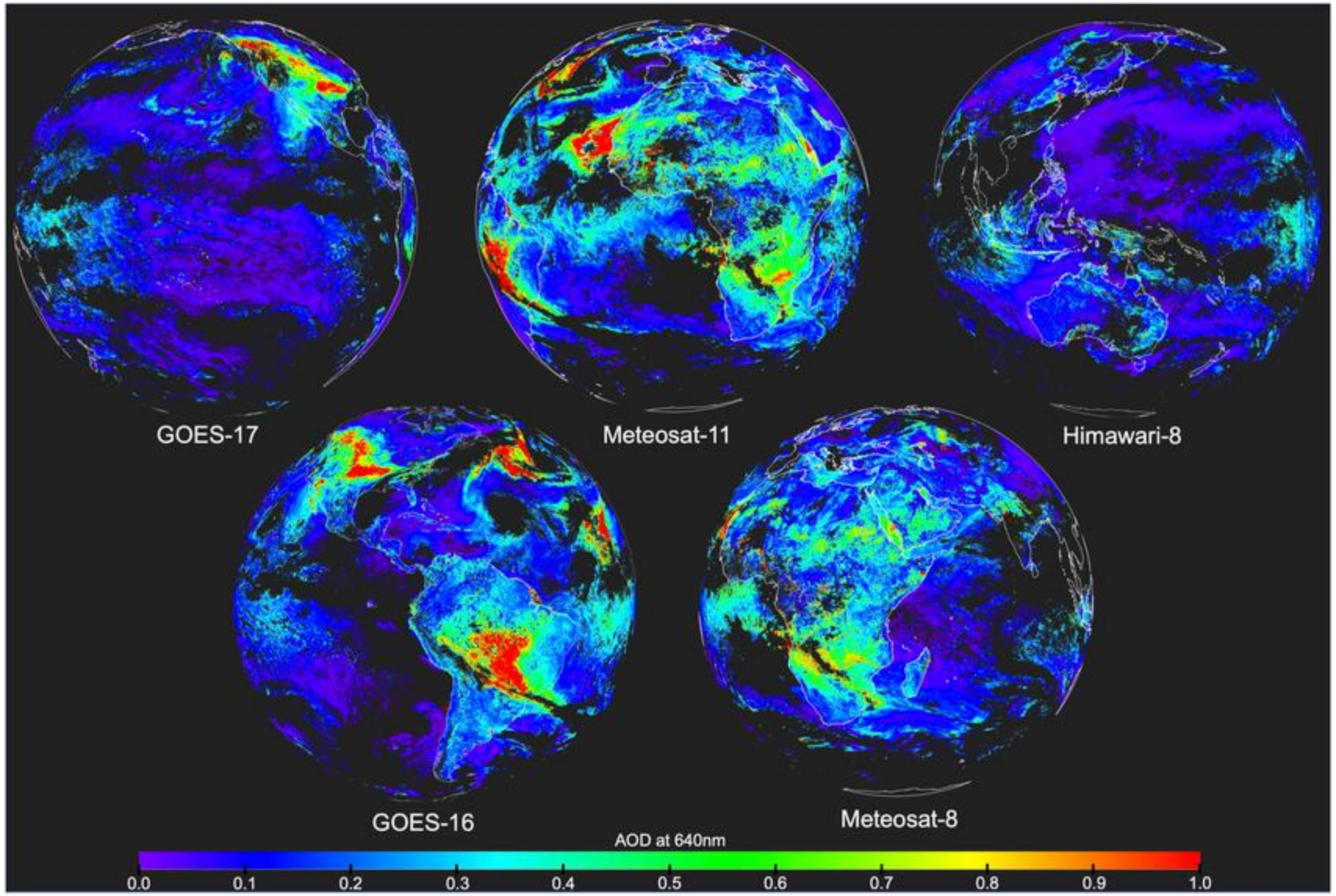

# Observations: infrared

On-board Polar-orbit Metop satellites (1, 2 and 3)

Aerosol product: AOD at 10um -> dust coarse particles

Day and night AOD

Algorithms: ULB, LMD, etc

12km (circular) pixel

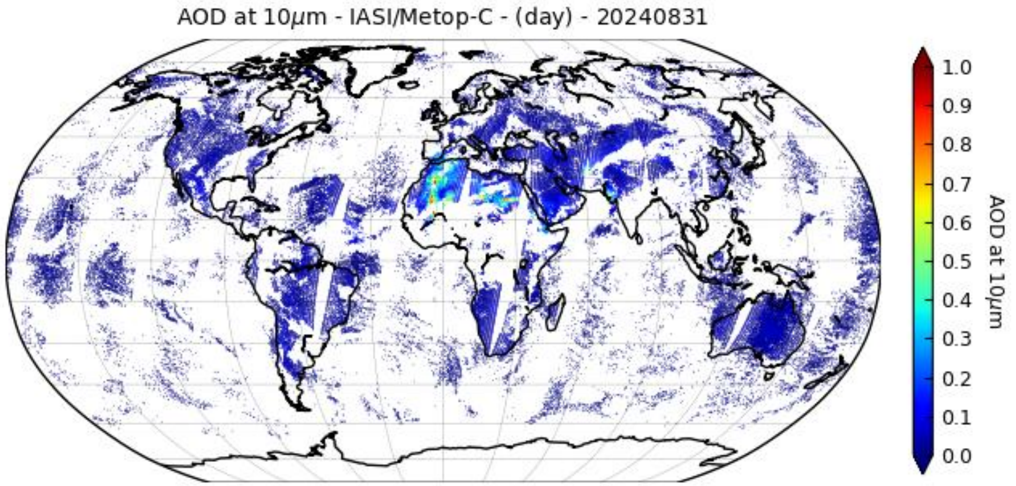


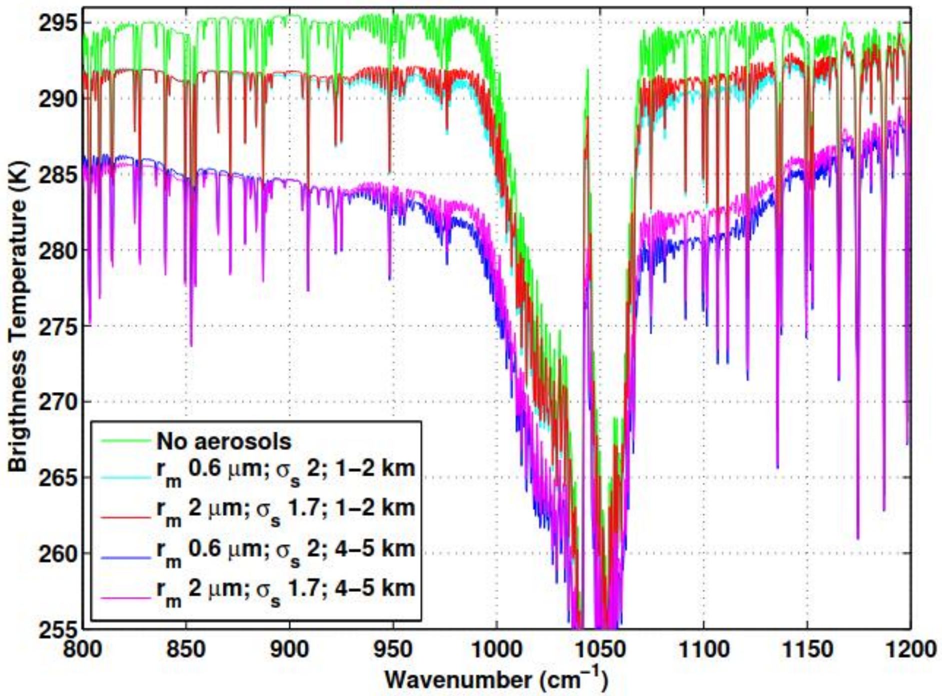


**Fig. 3.** Forward modelling of the radiance that would be observed by IASI for two particle size distributions associated with an aerosol layer at two different altitudes (optical depth of 1 at 10 µm). The corresponding forward modelling in absence of aerosols is also represented.

Vandenbussche et al (2013)

# Observations: UV

Residual method [Torres et al, 1998]: compares the observed UV spectral reflectance to that expected from a pure molecular atmosphere; any anomalous spectral contrast is attributed to UV-absorbing aerosols such as dust or smoke.

- ➢ Works over brigth surfaces and above clouds
- ○ Sensitive to altitude of dust layer
- ○ Qualitative index

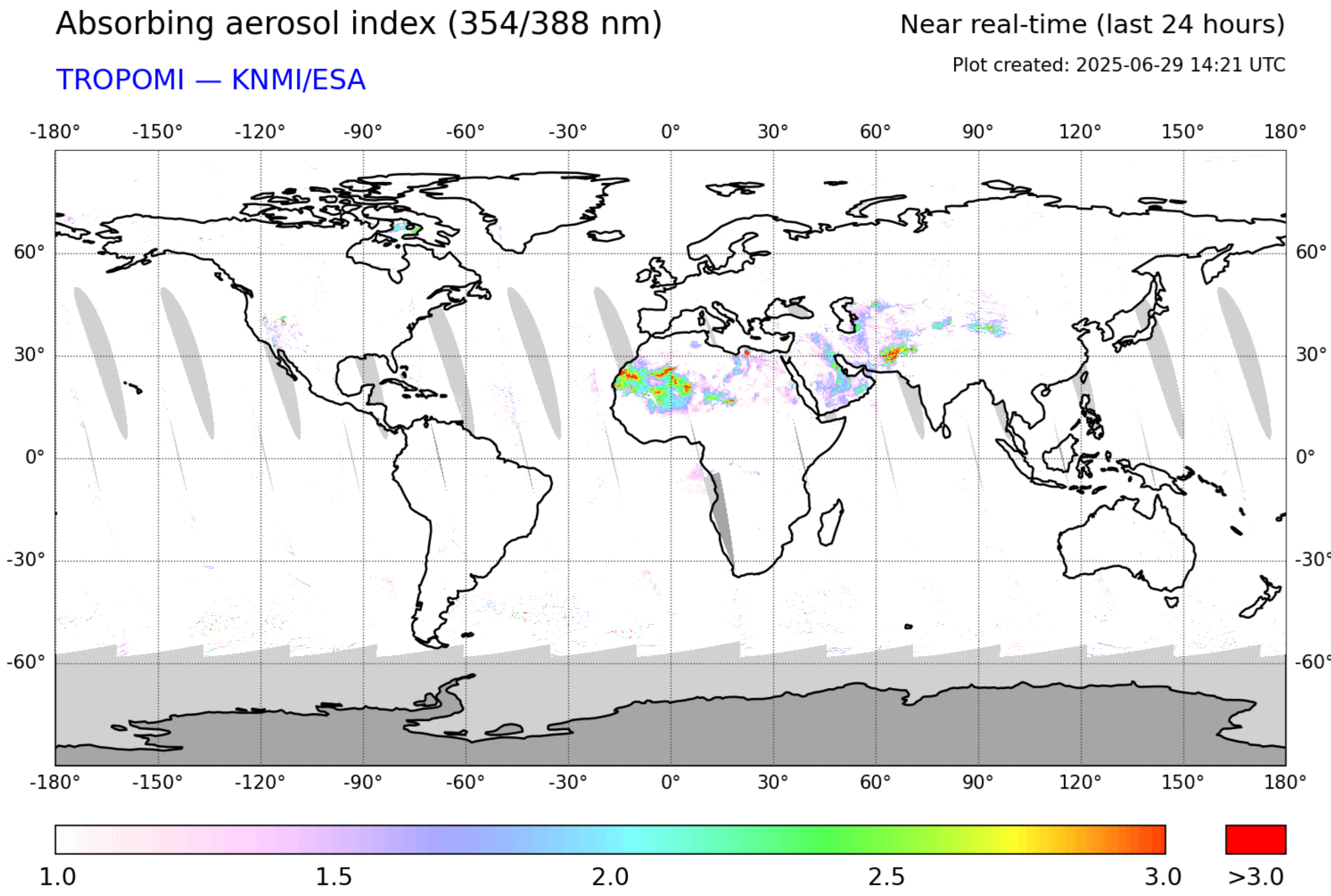

# Observations: LIDARS

**Cloud-Aerosol Lidar with Orthogonal Polarization (CALIOP)**:

2006-2023

elastic lidar (532 1024 nm) + depolarization (532nm)

Backscatter, extinction, aerosol typing

30m vertical resolution, 333m horizontal resolution

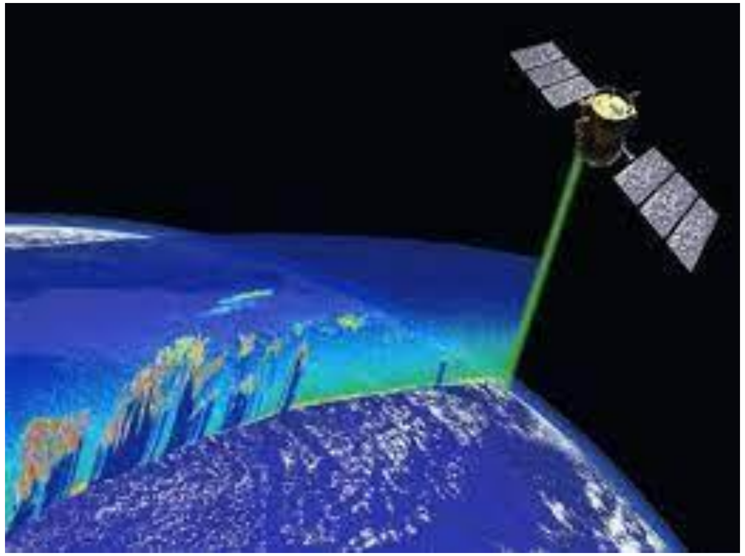

Can miss dust plumes due to long revisiting times (about 2 weeks)

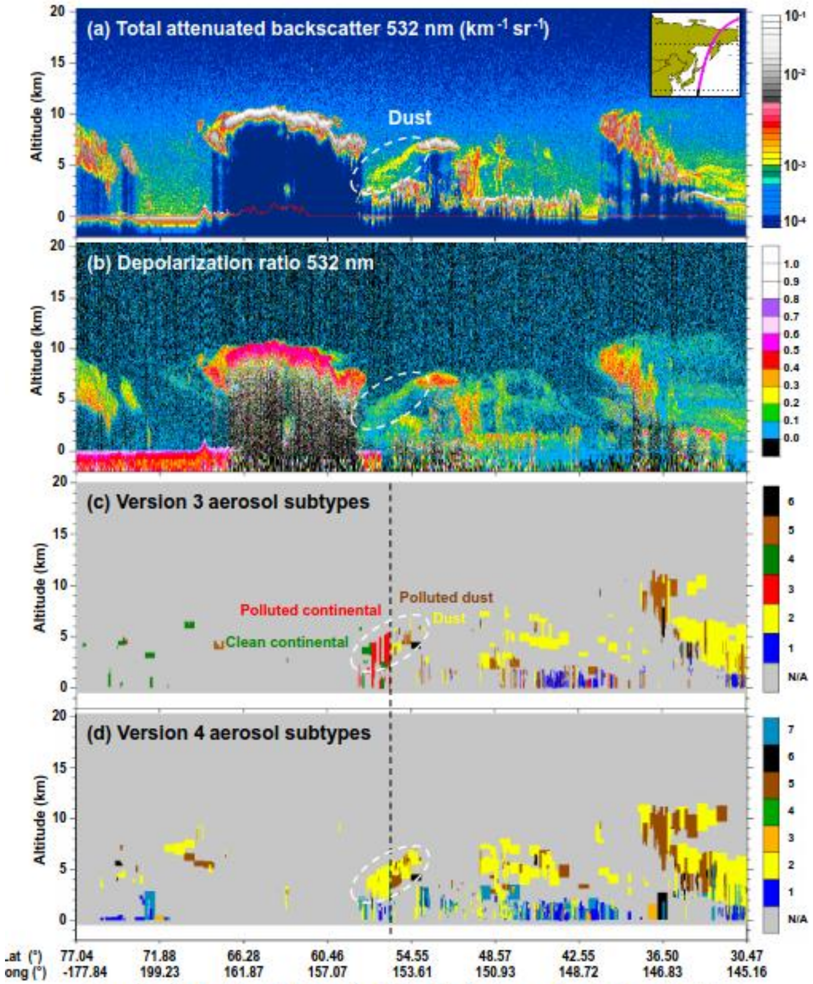

# Mineral dust assimilation: observations & control

- We never measure mineral dust directly but rather all aerosols combined
- We never measure aerosols mass / size distribution / composition from space directly but rather few extensive optical properties
- We best retrieve columnar amounts (AOD)
- It would be numerically expensive and not necessarily useful to define a control vector that is much more resolved than what we measure
- Some practical choices typically made for the control vector:
  - Columns of optical depth (2D)
  - Total aerosols mass concentration (3D)
  - Total aerosols extinction (3D)
- The unconstrained degrees of freedom follow the model prior

# Operational dust assimilation at BSC

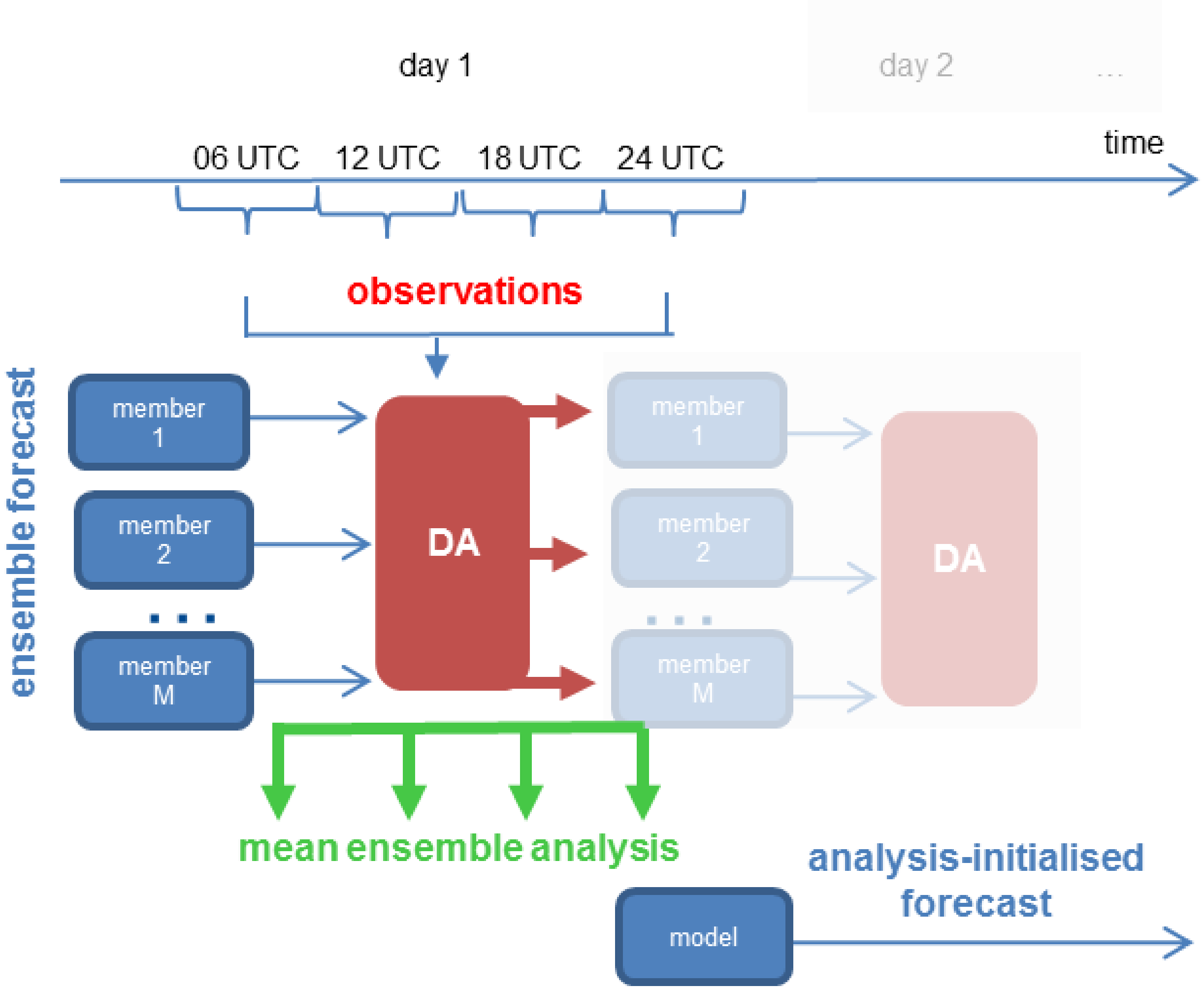

# Operational dust assimilation at BSC

**Experiment configuration: Ensembles**

Based in these five perturbation approaches :

***Retained for the o-suite***

- **FAC** : Random factor for dust emissions. One value per member.
- **BIN** : Random factor for dust emissions and threshold friction velocity of dust emission scheme. One value per member and dust bin.
- **MAP** : Random Gaussian correlated perturbation maps of emission factors. One map per member.
- **SCH** : Random linear combination of 4 dust emission schemes.
- **MET** : Meteorological initial and boundary conditions from ensemble forecasts (GEFS, Zhou et al., 2017)

*Escribano et al. EGU 2021*

- March and April 2017
- 20 members > reduced to 12 in the DA o-suite
- Assimilated: Dust optical depth (DOD) filtered from Deep Blue 550 nm AOD from VIIRS (SUOMI-NPP)

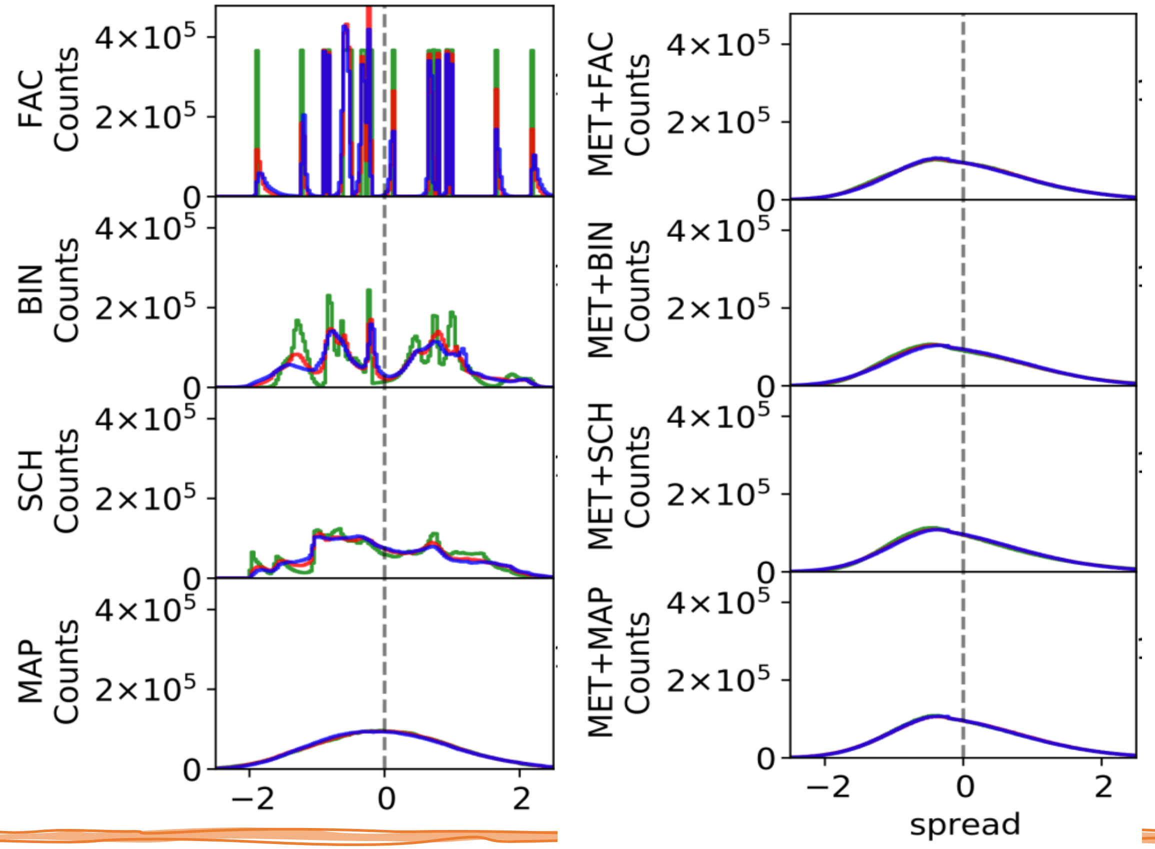


**fr** free run **fc** forecast **an** analysis

# Operational dust assimilation at BSC

**March 2025**

Aerosol Optical Depth at 550nm

Number of observations

All retrievals **QA**=3 ocean, **QA**=2 land

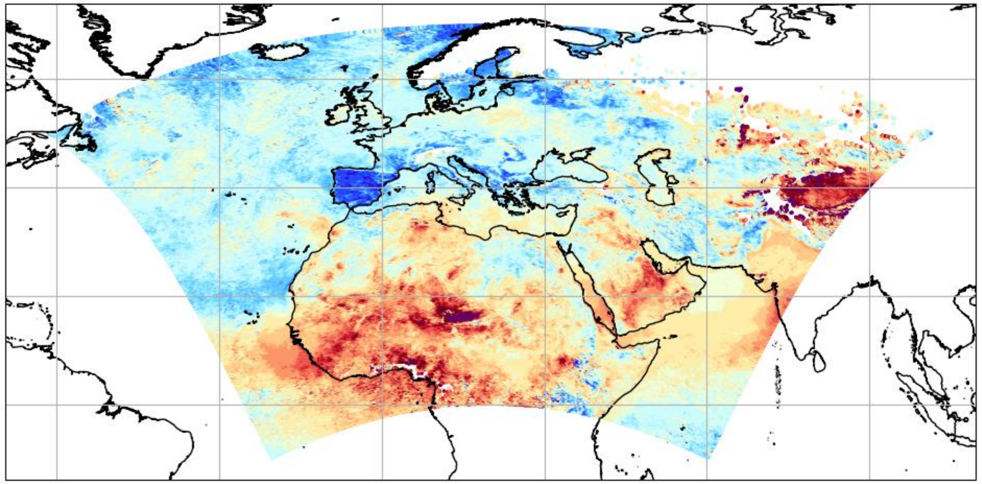

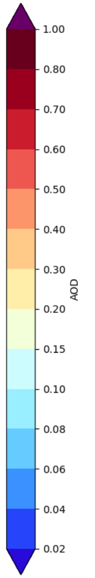


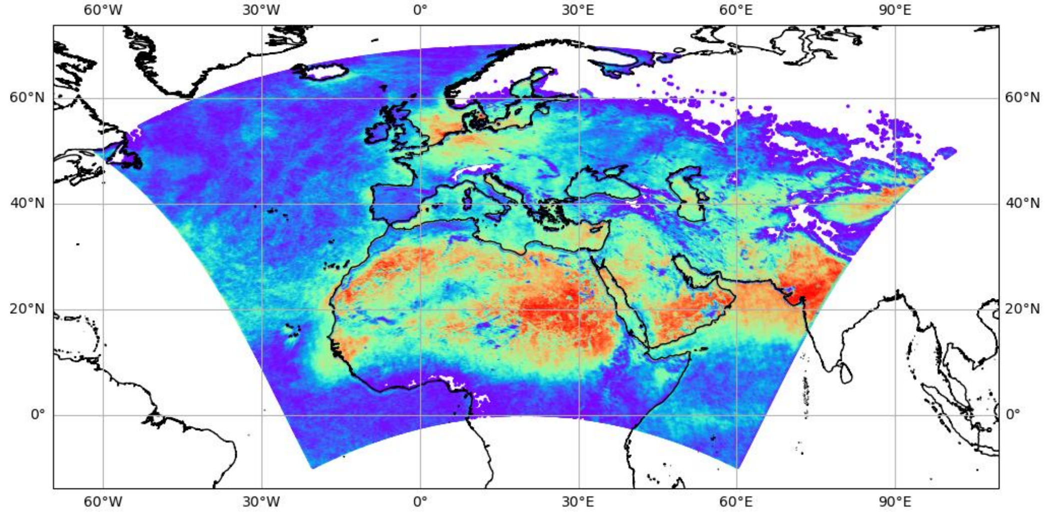


Dust flagged retrievals

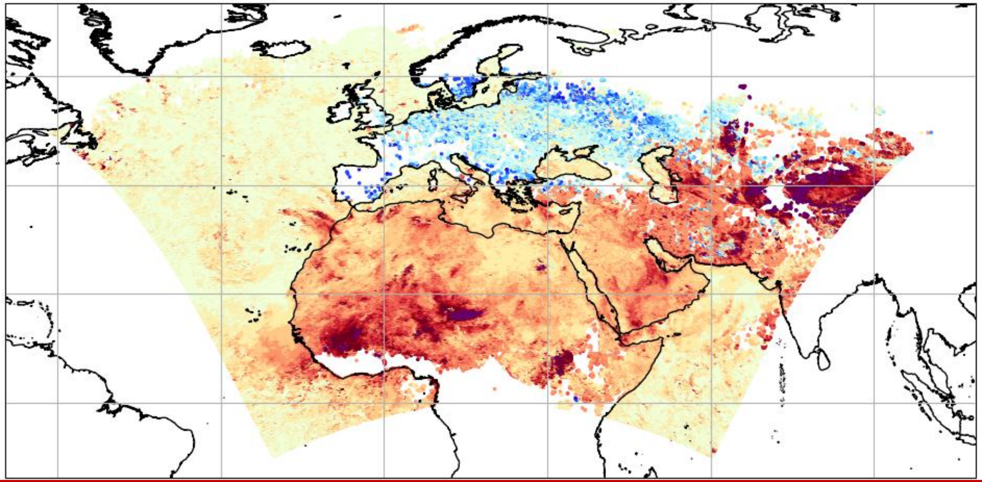

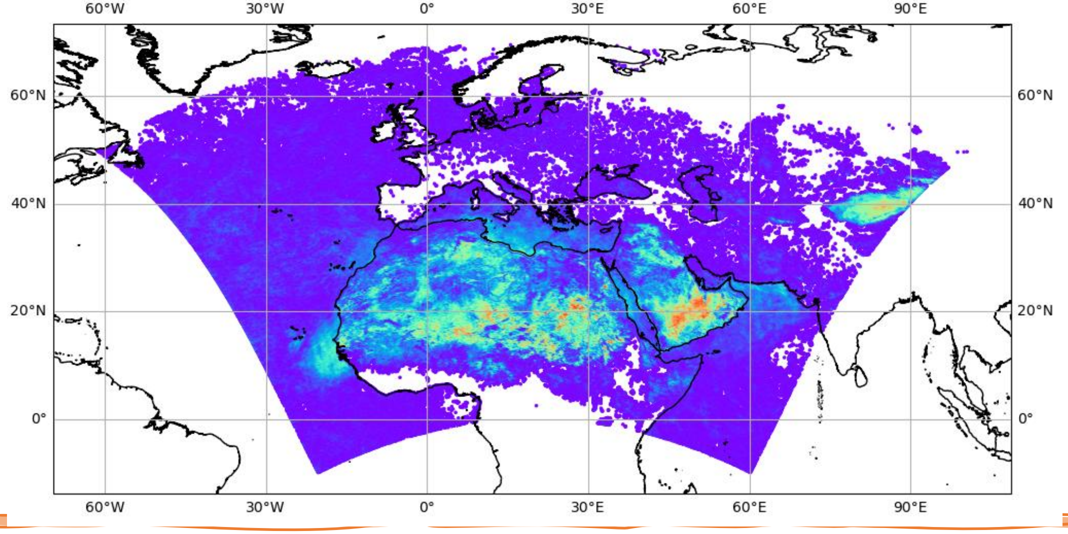


ERATOSTHENES CENTRE OF EXCELLENCE · BSC Barcelona Supercomputing Center Centro Nacional de Supercomputación · GRASP · ARMINES · MINES PARIS | PSL · Ciências ULisboa · FCiências.ID · pmod wrc

# Operational dust assimilation at BSC

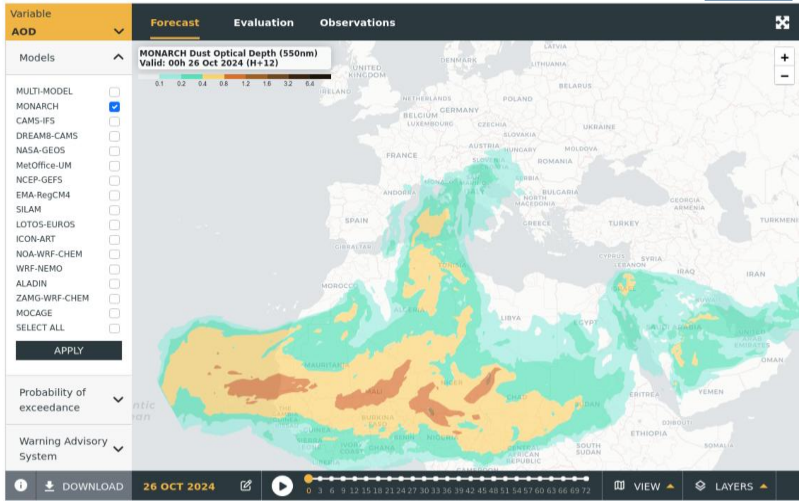


| SDS-WAS MONARCH | Configuration |
|---|---|
| **Meteorology** | Inline<br>NMMB |
| **Initial and boundary conditions** | GFS 0.5x0.5 deg |
| **Resolution** | 10 km |
| **Levels** | 40 |
| **Forecast range** | 3 days |
| **Output frequency** | 3 hours |
| **Species** | Dust |
| **Size Bins** | 8 (0.2-20 µm) |
| **Dust sources** | MODIS Col. 6 Deep Blue FoO clmatology (Ginoux et al. 2012) |
| **Emission scheme** | Modified GOCART scheme (Klose et al. 2020) |
| **Radiation scheme** | Coupled online with dust |

| Data assimilation | Configuration |
|---|---|
| **Algorithm** | LETKF-4D |
| **Assimilation window** | 24 hours |
| **Time step** | 3 hours |
| **Observations** | NOAA20 VIIRS Deep Blue Dust Flagged AOD |
| **Observation errors** | 0.05 +- 0.2AOD |
| **Ensemble size** | 12 members |
| **Ensemble perturbations** | Global and spatially correlated emission perturbations |
| **Control vector** | Total dust mass (3D) |
| **Localization radius** | 150 km |

# Operational dust assimilation at BSC

October 2024

January 2025

May 2025

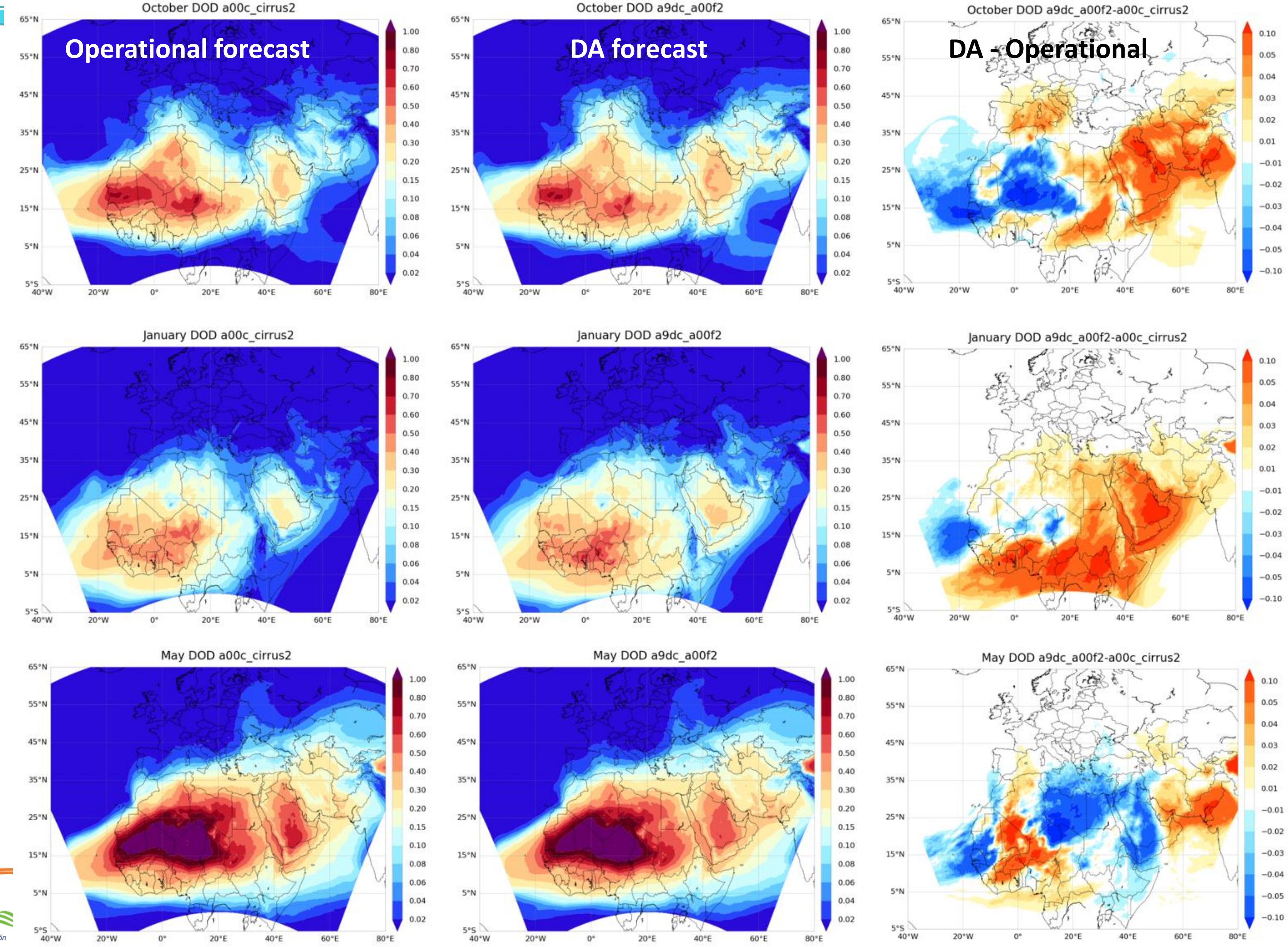

# Operational dust assimilation at BSC

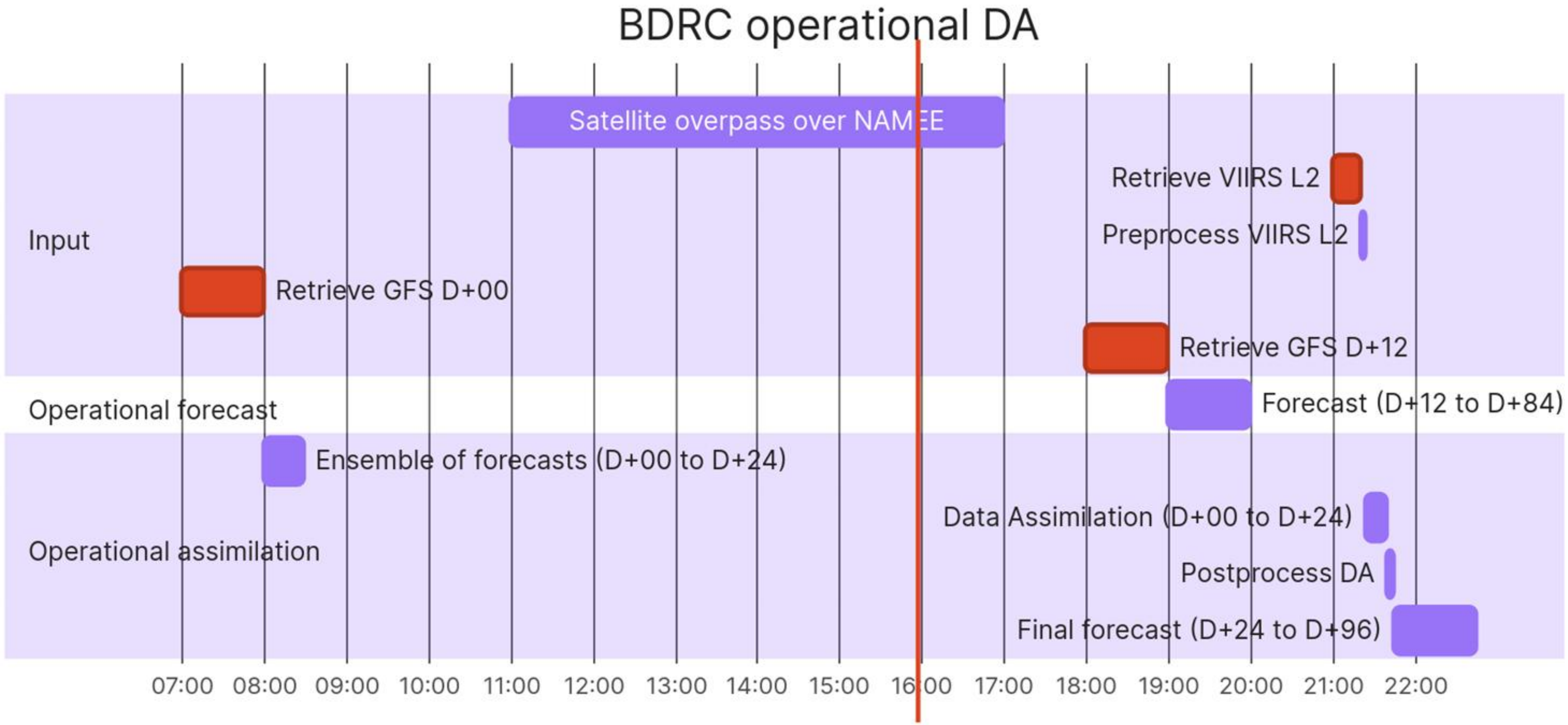

# Mineral dust assimilation: reanalysis skills

- The analysis is the closest we can get to the truth (assuming DA was well tuned and systematic biases were not too large)
- We need to evaluate it against independent set of observations
- Time series of latest MONARCH reanalysis processing (red) versus AERONET L2 Coarse AOD in 2018-2019

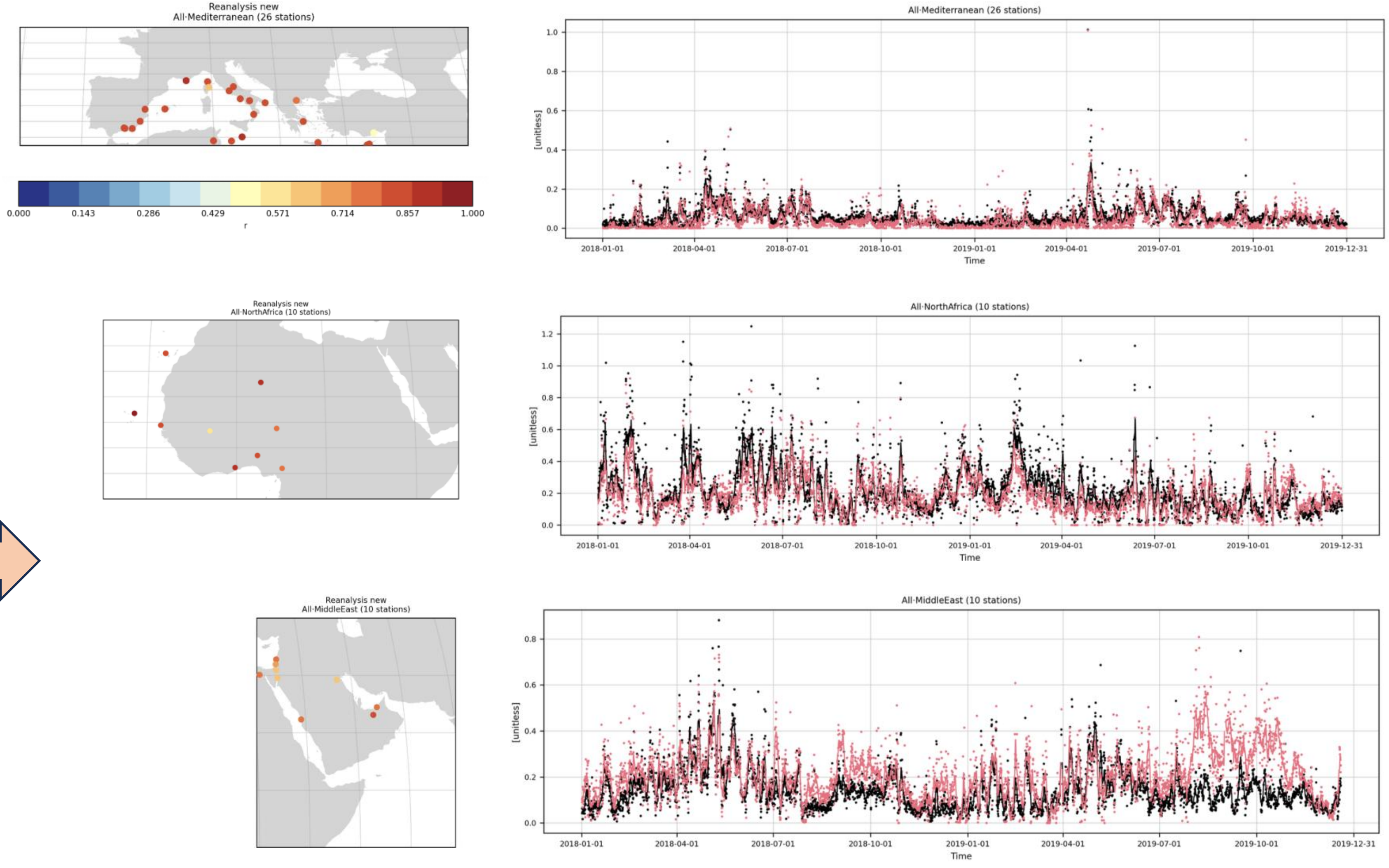

# Mineral dust assimilation: forecast skills AOD

| | Center | Assimilation |
|---|---|---|
| Oper Forecast (o-suite) | BSC | None |
| DA Forecast (e-suite) | BSC | VIIRS |
| GEOS | NASA | MODIS, AERONET |
| UM | UK Met Office | MODIS |
| CAMS | ECMWF | MODIS, VIIRS, PMAp |
| MOCAGE | Meteo France | MODIS, VIIRS |
| SDS-WAS | BSC | Median of 14 models, 4 with DA |

AERONET L1.5 **Direct Sun AOD** at 550 nm versus modeled **Dust Optical Depth** at 550 nm, filtered with **AE < 0.6**, 3-hourly frequency

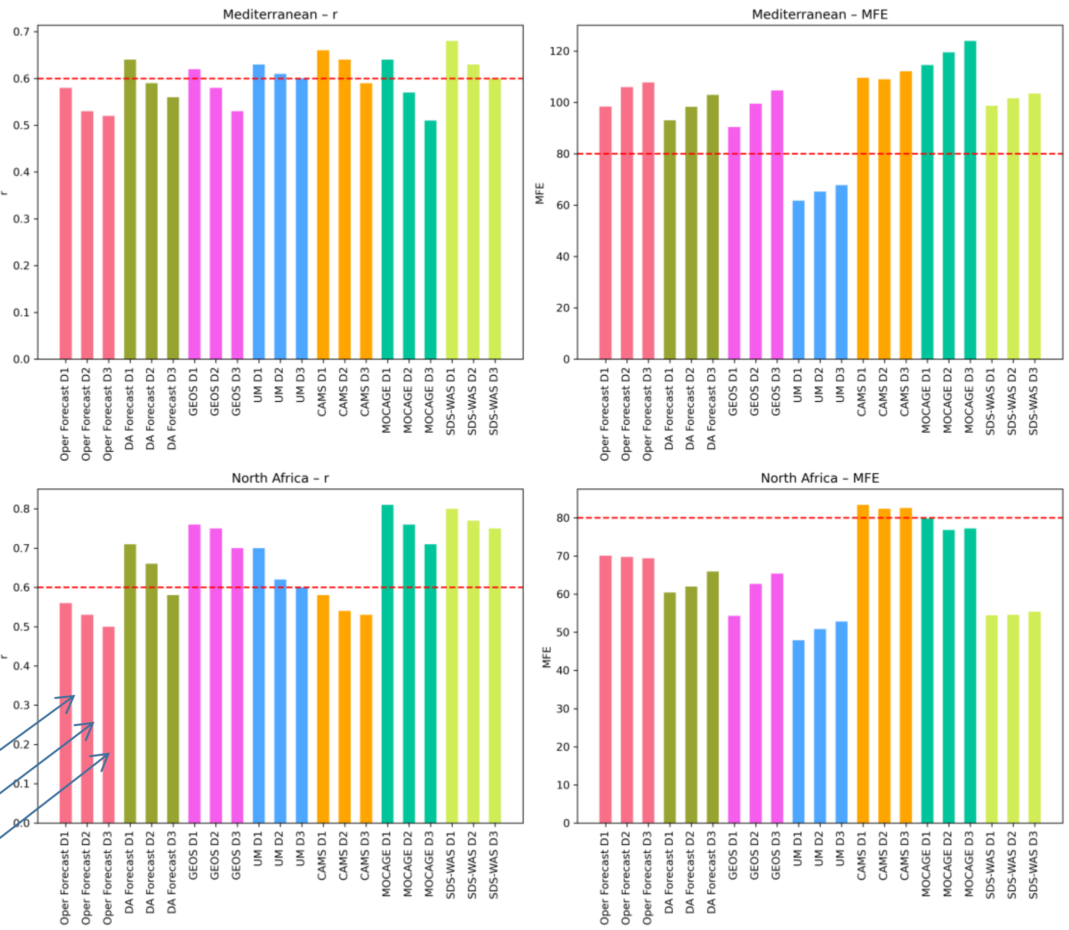


**D1 D2 D3**

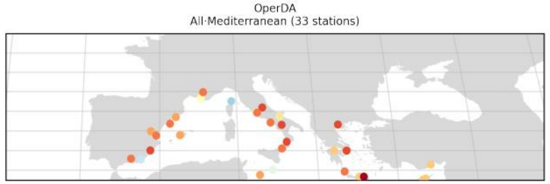


r

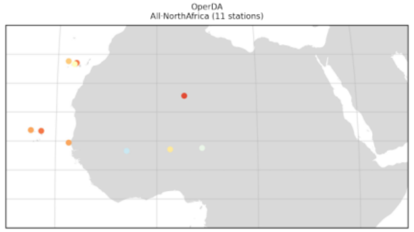

# Mineral dust assimilation: forecast skills surface

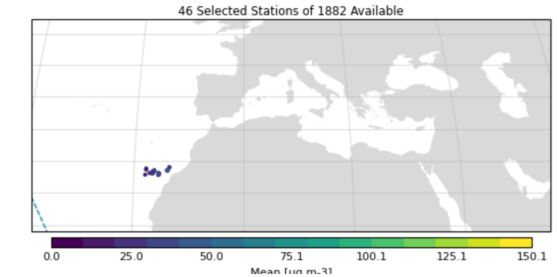


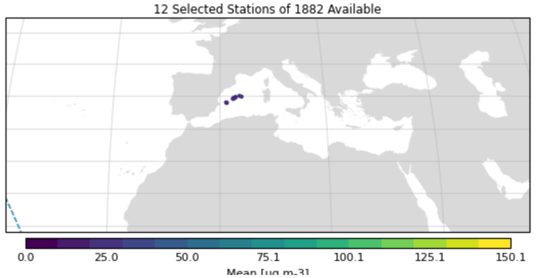


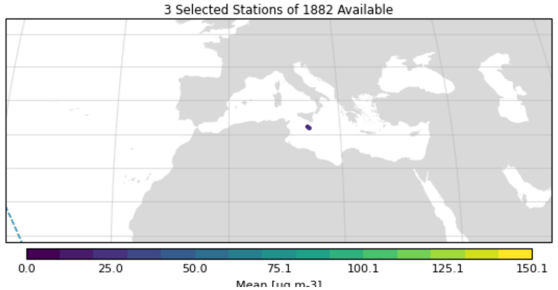


Approximation: total dust concentration versus all aerosols < 10 µm

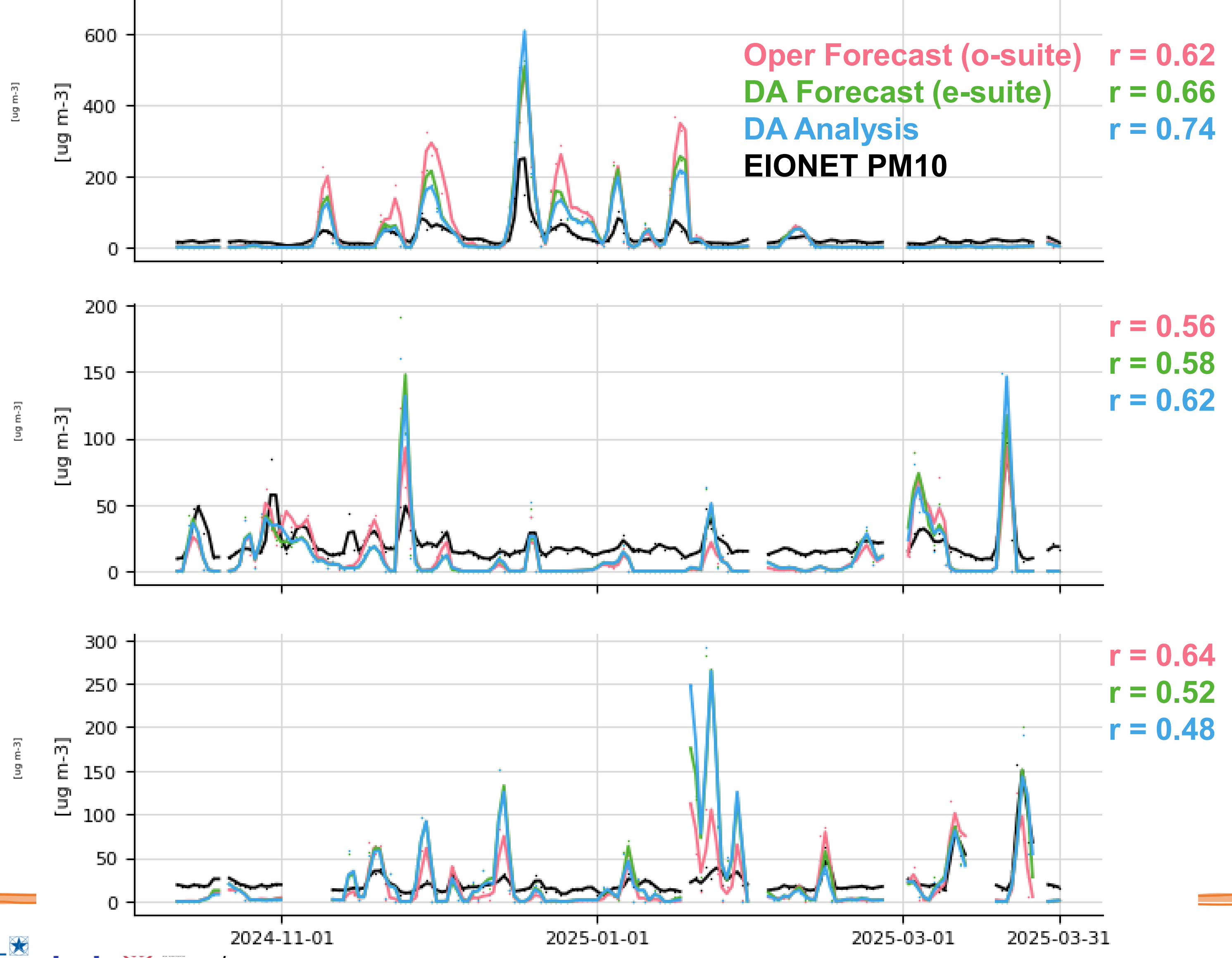

# Mineral dust assimilation R&D

# Satellites era transition

Courtesy of J. Reid (ICAP 2024)

- MODIS served extremely well aerosol assimilation systems for more than a decade but is getting retired very soon

- Now moving to current generation of visible sensors
  - NOAA VIIRS for the afternoon overpass
  - EUMETSAT Sentinel 3 for the morning overpass

- Retrieval quality can differ substantially among sensors and even among algorithms using the same sensor!

- A lot of work to ensure that this transition will be smooth

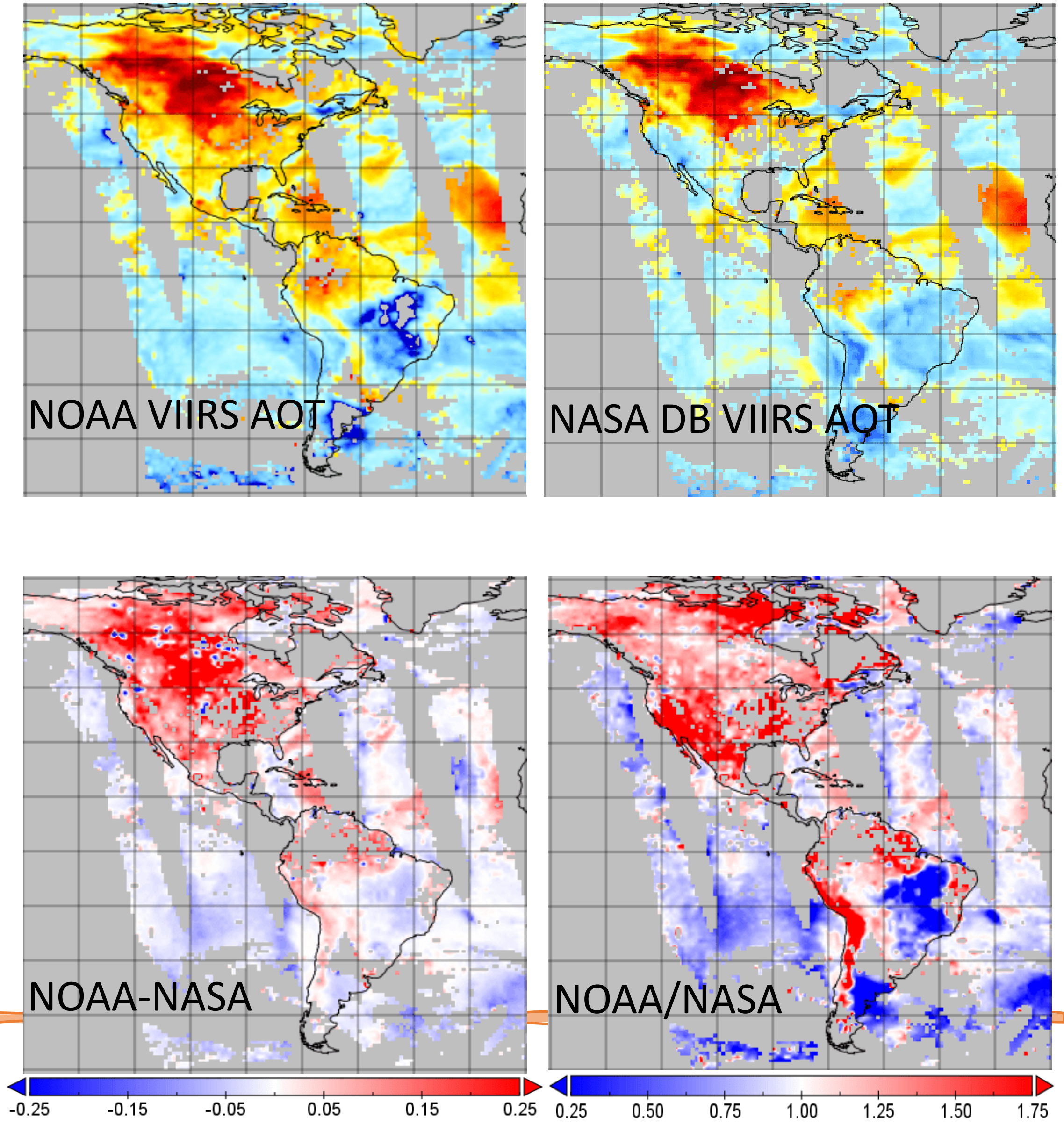

# Infrared assimilation

Courtesy of M. Ades (ICAP 2024)

Atmosphere Monitoring

## IASI ULB coarse particle retrieval

- Dust was advected from the Sahara across Europe in Feb 2023
- Distinctive dust plume across the UK on the 15th Feb 2023 captured by AOD but attributed partly to sulphate
- IASI optical depth at 10um retrieval is being explored to see if it can help with the speciation of the aerosols
- Using the OD10 retrievals together with AOD brings improvement

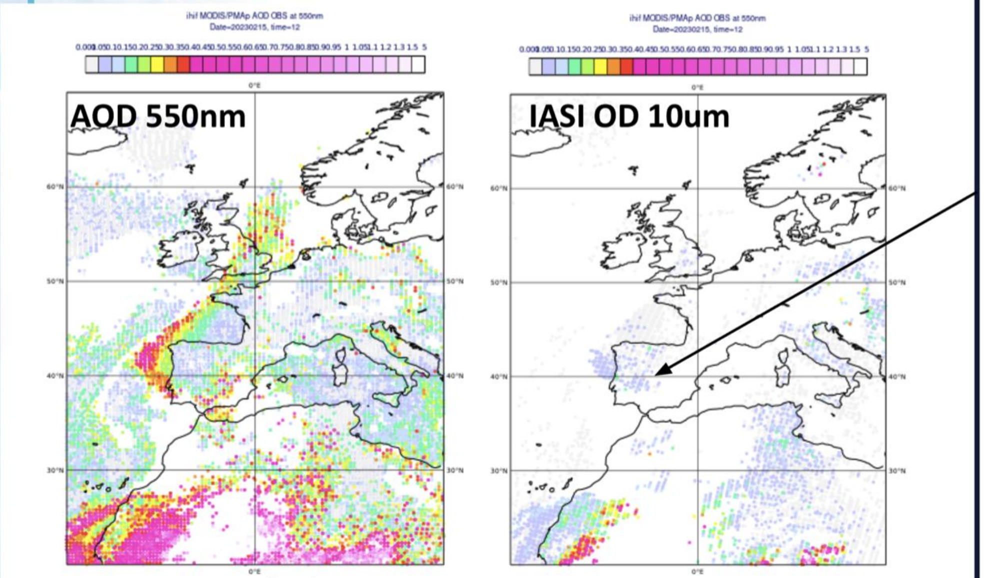


Aerosol observations on 20230215

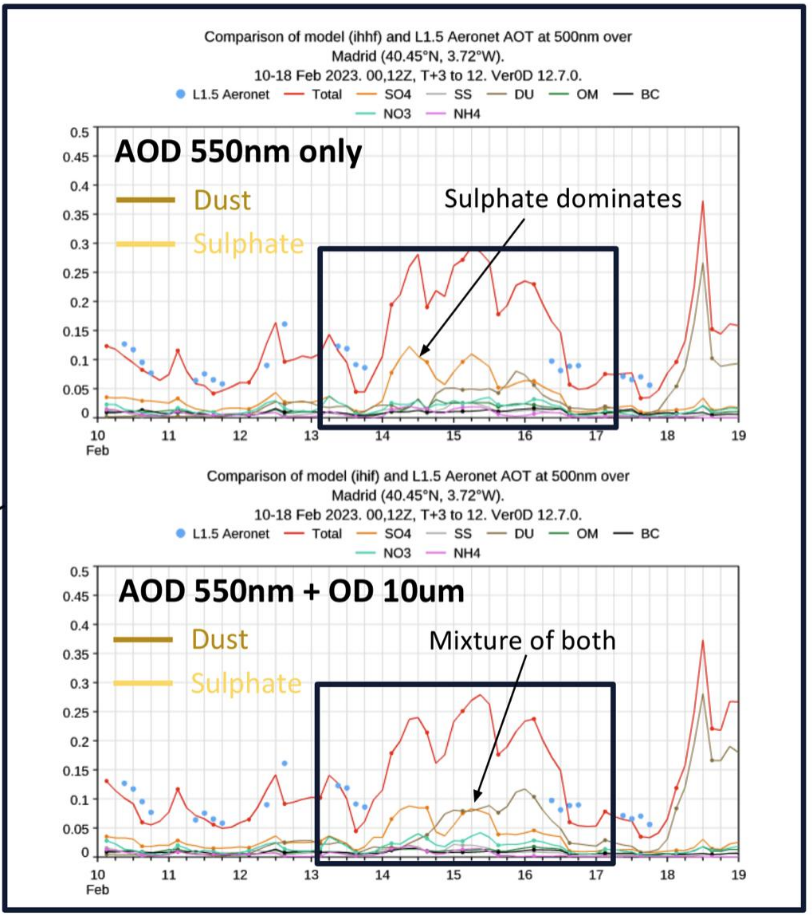

# LIDAR assimilation

Courtesy of M. Ades (ICAP 2025)

PROGRAMME OF THE EUROPEAN UNION | Copernicus Europe's eyes on Earth | Atmosphere Monitoring Service atmosphere.copernicus.eu | IMPLEMENTED BY ECMWF

## EarthCARE

- ATLID **aerosol backscatter** provides a new vertical constraint on aerosol profiles for atmospheric composition models in both day and night.
- As part of EarthCARE DISC, feasibility studies are being performed for monitoring and assimilation of L2 aerosol products.

2025-03-31 1600 UTC (4772D, 4772E)

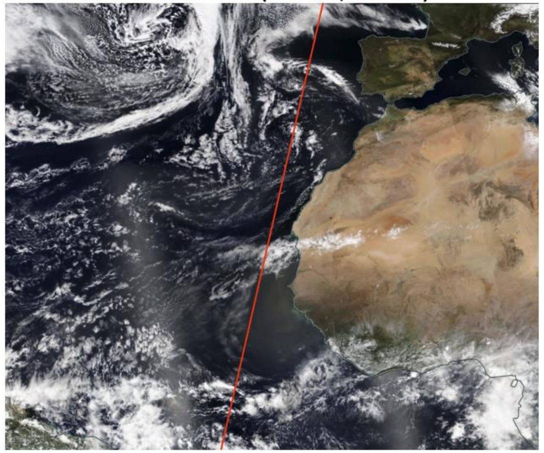

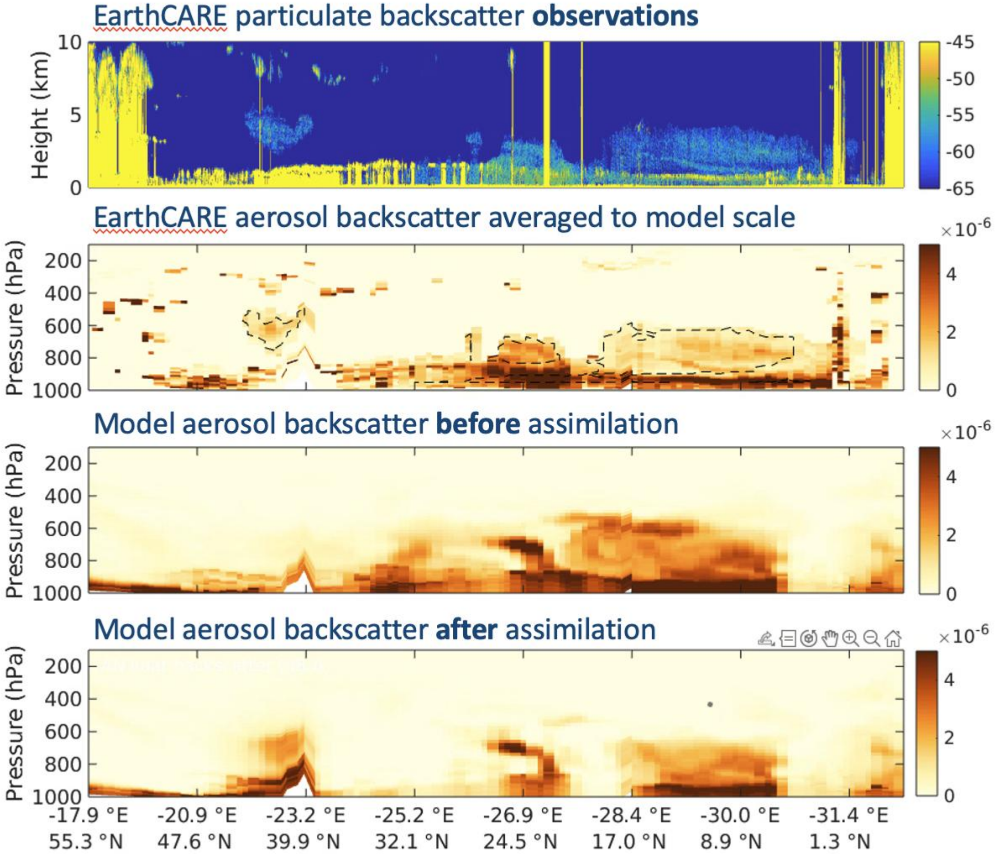


*Thanks to Will McLean and Mark Fielding*

# Multi-instrument assimilation

Courtesy of G. Monteil

## Do satellite AOD retrieval help modelling (and forecasting) surface air quality?

The MONARCH-DA system:

- NMMB-MONARCH model: **7 aerosol species, with 1-7 bin/species**
- LETKF data assimilation algorithm
- Joint assimilation of **surface PM10** observations and **VIIRS 550 nm total AOD retrievals**

Experimental setup:

- One month assimilation, in January 2024
- 6-member ensemble (i.e. operational CAMS setup)
- “offline” assimilation (no propagation of the analysis)

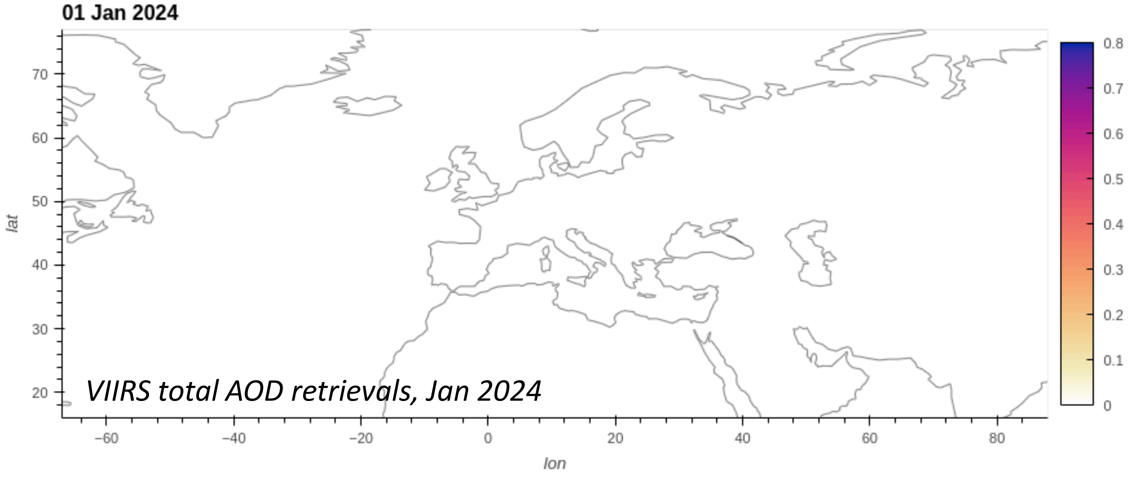


*VIIRS total AOD retrievals, Jan 2024*

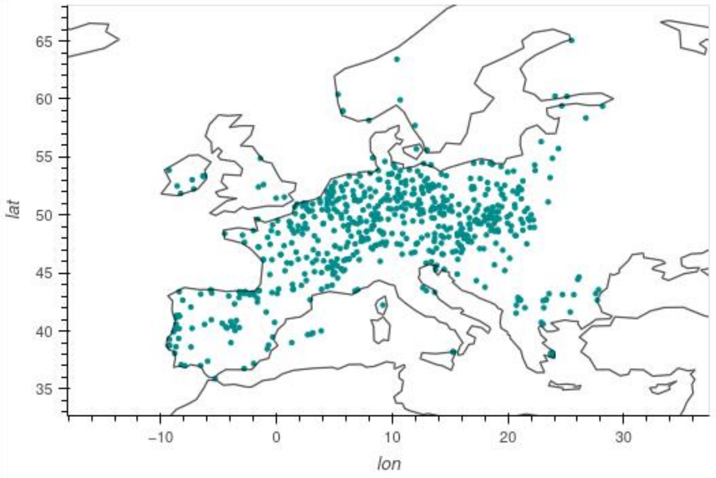


*Surface observation sites (validation sites in red)*

# Multi-instrument assimilation

Courtesy of G. Monteil

- MONARCH-DA is capable of jointly assimilating surface and satellite observations of aerosols
  - Fit to both obs datasets is improved
  - The DA is capable of accomodating both constraints by small adjustments in the vertical profiles, when needed.

- So far, this doesn’t translate into measurable improvements in surface air quality estimates

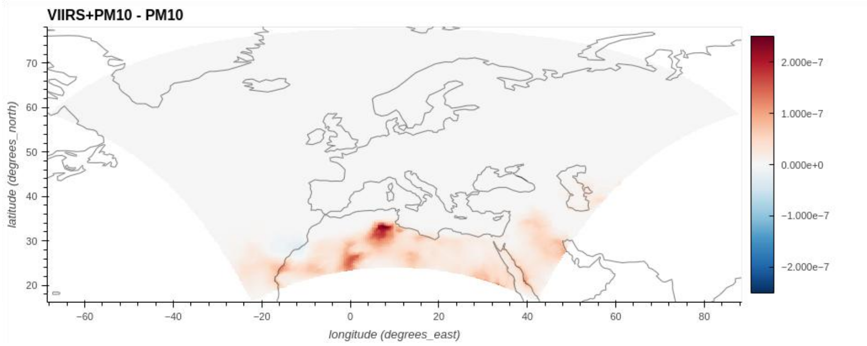


*Difference between DA of VIIRS+PM10 and DA of PM10 on surface PM10 levels (jan 2024 average)*

*Fit to VIIRS AOD*

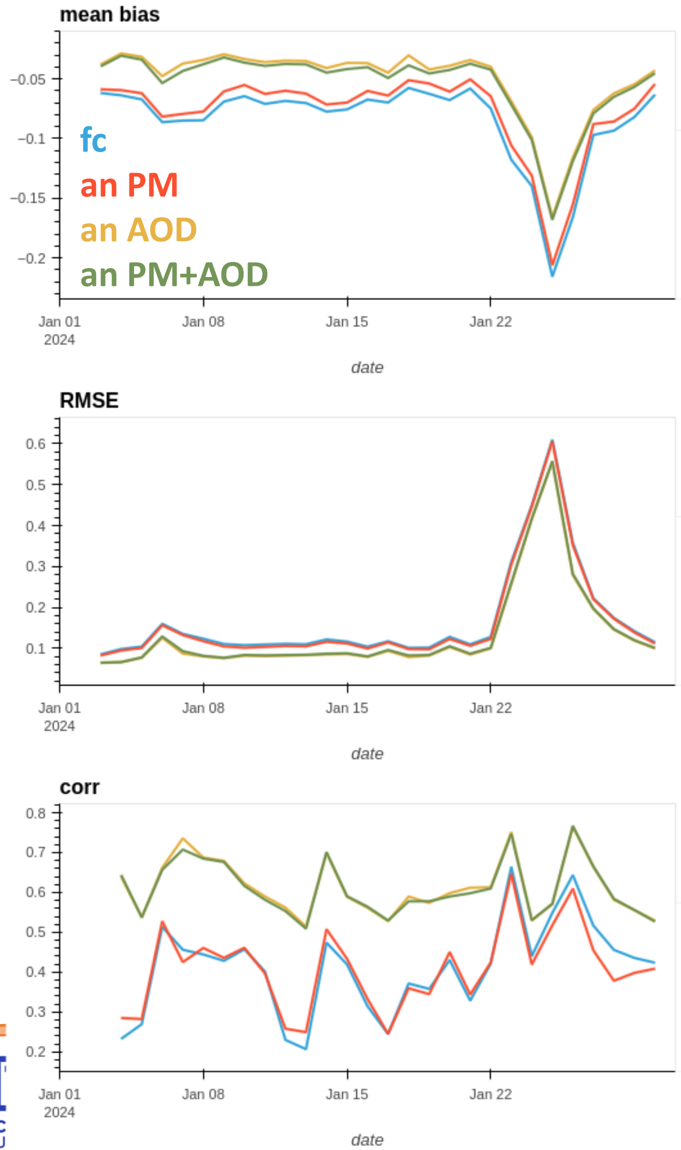


*Fit to EIONET PM10*

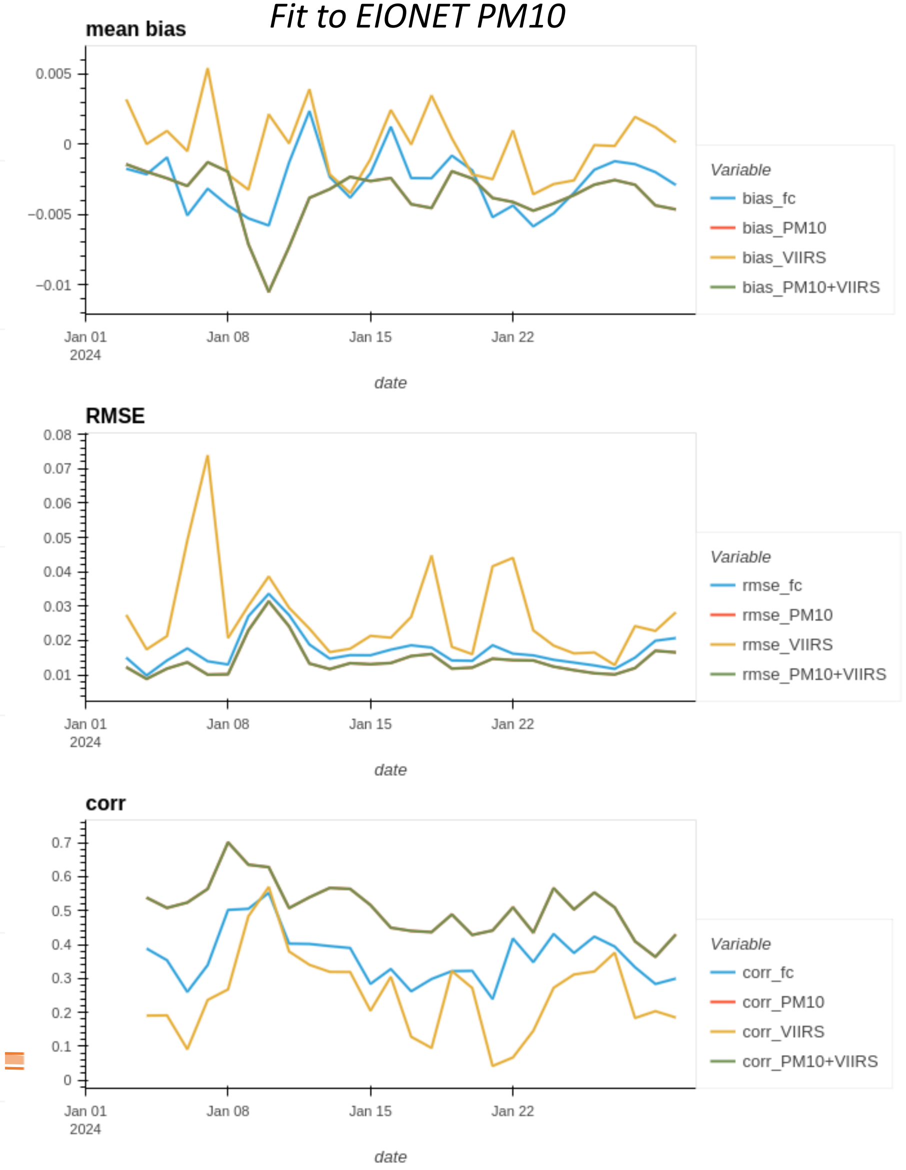

# Radiances assimilation

Courtesy of S. Quesada-Ruiz (CAMEO 2025)

## Aerosol visible assimilation case study – dust event 4 June 2025

**First Guess Simulated Reflectance**

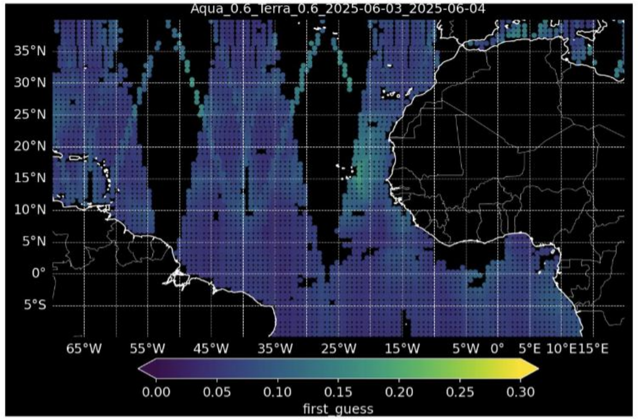


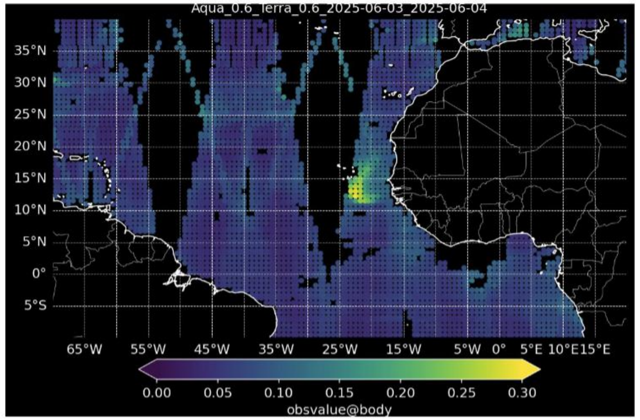


**MODIS Observations**

**Analysis Increment**

orange = increase AER
purple = decrease AER

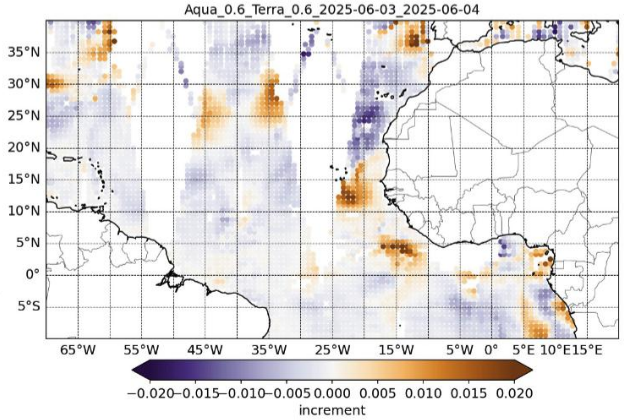


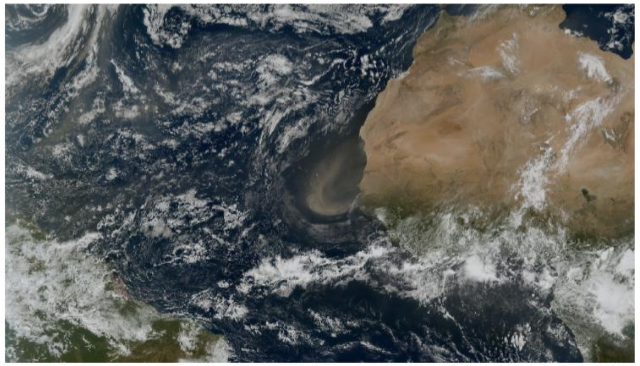

https://www.eumetsat.int/saharan-dust-over-atlantic-ocean

**Independent FCI composite observation showing the dust outbreak**

# Dust emissions inversion

Courtesy of J. Escribano

1. Readapted the LETKF algorithm to estimate temporally and spatially varying emission fluxes
2. Dust emissions correction factors evaluated for 2017-2021

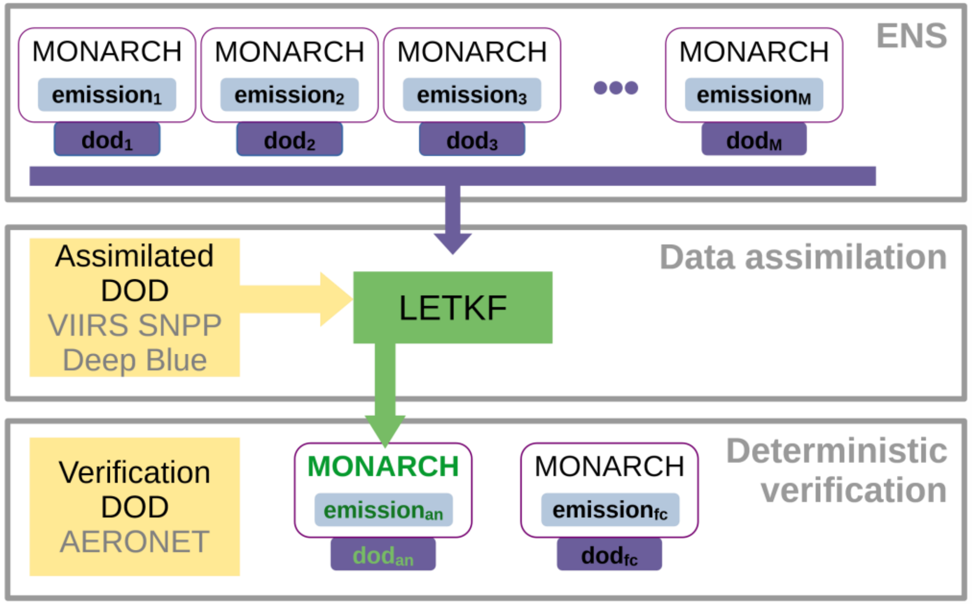


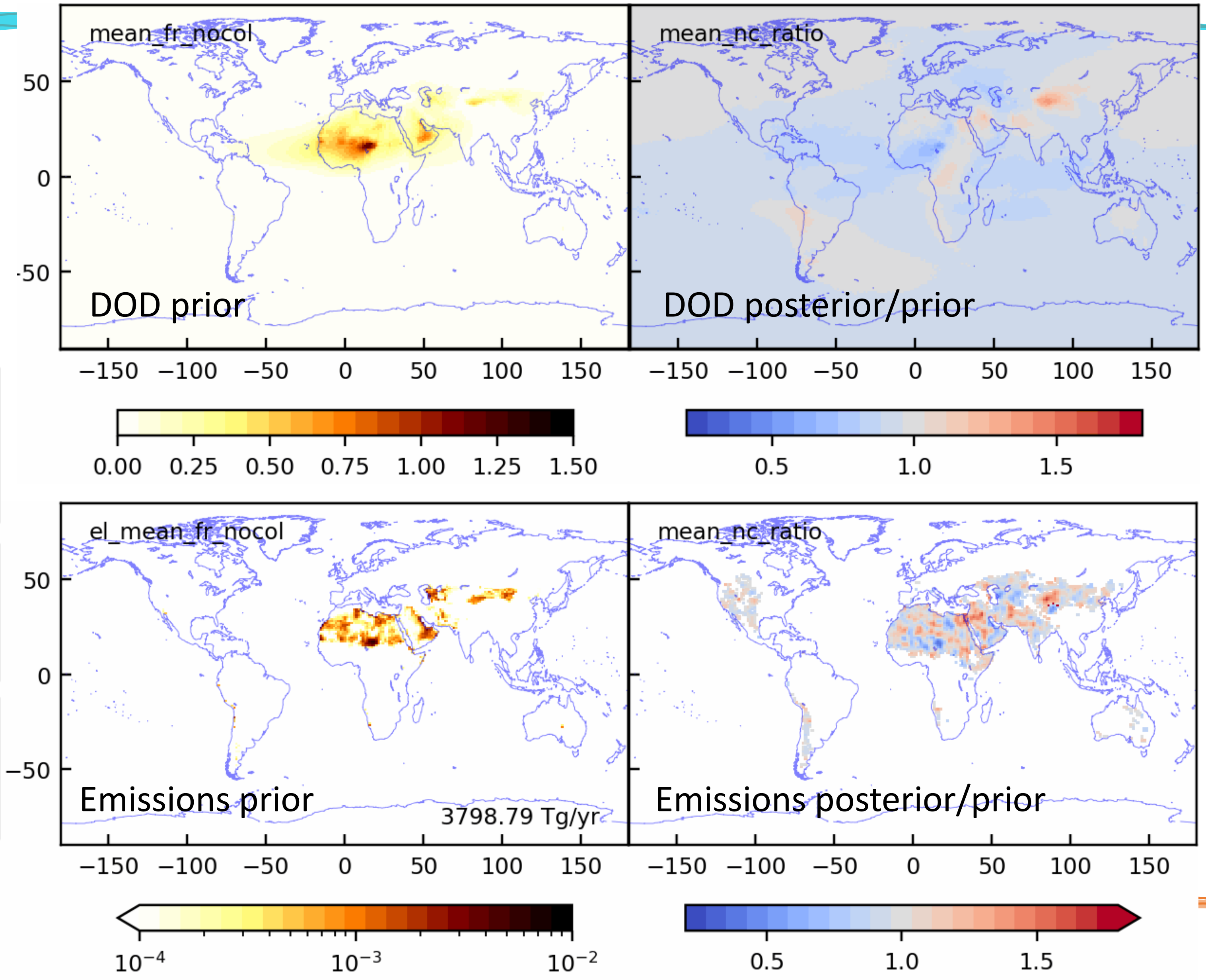

# Final remarks

- Data Assimilation (DA) became a cornerstone of aerosols forecasting (thanks to the success story of MODIS)

- DA fundamentally produces a weighted average between a model prior and observations, but correctly distribute corrections across the multi-dimensional model state according to relative uncertainties. The state can also be the dust emissions!

- Variational methods rely on linearized operators , ensemble methods on sampling the observations sensitivities. Many / different nature of observations might favor first in the long term, but still to be proved.

- Mineral dust observations from space are very different from typical models state variables. The accuracy of the observation operator plays a lot. Producing relatively good optical depths does not ensure improved mass concentrations.

- Many opportunities with recent and upcoming satellites, but how to reconcile systematic biases across satellites / observation operators?

- DA still only corrects initial conditions in mineral dust forecasts. This is a strong limitation to forecast improvements -> Machine Learning / AI to tackle model errors?

# References


1. ECMWF Data Assimilation course: https://events.ecmwf.int/event/376/timetable
2. To be completed…

Funded by the
European Union

# THANK YOU

*This project has received funding from the European Union's Horizon Europe Framework Programme under the grant agreement No 101160258. Views and opinions expressed are however those of the author(s) only and do not necessarily reflect those of the European Union.*